Technische Hochschule Ingolstadt
Fakultät für Maschinenbau

Faculty of Mechanical Engineering

Renewable Energy Systems (RES)

Master Thesis

Analysis of DC Charge Distribution and Electromagnetic Fields in High-Voltage Direct Current Transmission Lines for Bulk Energy Transmission

Mohamed Samy Abdel Moaty Refaay

Matriculation Number: 00086753

Academic Supervisor (first examiner): Prof. Dr.-Ing. Daniel Navarro

Academic Supervisor (Second examiner): Prof. Dr.-Ing. Tobias Schrag

Technische Hochschule Ingolstadt (THI) Ingolstadt, Germany, 2021

Abstract

High-voltage direct current (HVDC) transmission systems continue to develop over time. Because primarily and only dependent on high voltage alternating current (HVAC) transmission lines, can cause some constraints on installation costs and technical considerations in some cases. A comparison between the two systems is important in order to highlight the properties of the individual systems. The comparison shows the suitable conditions to replace an HVAC system with an HVDC system in terms of economic, technical and environmental assessments. This work discusses the different types of HVDC transmission technologies and their applications. Specification of the components of the HVDC transmission system and the practical implementations of such a system with different transmission medium topologies. The feasibility of setting up a reliable HVDC transmission system depends on the power electronic devices and thus opens the way for the implementation of various projects and the possibility of operating the system smoothly and with a high degree of controllability. The applications of the HVDC transmission system are presented with a discussion of the properties of HVDC power cables and current distribution. In some cases, hybrid HVDC-HVAC transmission lines share the same transmission tower and therefore electromagnetic interference occurs. Designing a transmission system is based on determining the amount of power desired to be transmitted thus the standard line voltage is selected. Then the line current can be computed and hence sizing the cable is necessary to meet the system requirements. A case study is analyzed and calculated which represents a methodology of sizing power HVDC cables.

Keywords: HVDC transmission, DC power links, HVDC XLPE cables, power electronic devices, sizing DC conductor, ampacity cable, HVDC system

Acknowledgment

First of all, I would like to express my sincere gratitude to my supervisor Prof. Daniel Navarro for his consistent support and guidance in carrying out this work. Thank you for continuously giving me your fruitful feedback on my thesis and for always being ready to support me in any way throughout the research project. I have really appreciated your support, expertise and guidance.

Furthermore, I would like to thank the Faculty of Mechanical Engineering at the Technische Hochschule Ingolstadt and all the staff of its members for providing the course of renewable energy systems, which helped me to gain more experience in this field.

Finally, I want to thank my family; Mother, father, brother and sister as well as my friends who looked after me and encouraged me in difficult situations. Thank you so much for your prayers, trust and faith in me.

Table of contents

List of Figures

List of Tables

1 Introduction

HVAC systems are known for their reliability and low cost in terms of generation, transmission and distribution. However, the transmit of bulk power from remote areas depending on HVAC lines can cause some problems. HVDC transmission systems tend to be the preferred ones, especially in view of the steadily growing power rate consumption worldwide. The reason why the generation and transmission facilities have to increase the capacity to cover all loads and the orientation towards the construction of power plants that run on renewable energy resources and in many cases can be very far from the distribution regions. For example, for hydropower plants that are out of control regarding their locations, which may be hundreds of kilometers from load centers, environmental considerations also play a role in the placement of the generation point [26]. The main difference that determines whether the choice of a transmission medium is AC or DC and to be economically and technically efficient is the transmission distance. The integration of power electronic devices, especially the high-voltage controlled semiconductors, has contributed to the development of HVDC transmission technologies over time. In addition to the ability to transmit mass power over long distances with a high level of power flow control and system stability.

The first section of this paper discusses a comparative assessment between HVDC and HVAC transmission systems, showing that the main variables define the superiority of each system over the other. In general, the focus of this work is on the HVDC transmission system. Therefore, the first section is followed with defining the HVDC technologies and the system components on the basis of the power electronic devices that are illustrated as well.

The 2nd section focuses on the different topologies according to the DC link type, which can be divided into three types of monopolar, bipolar and multi-terminal topologies. Multi-terminal-based HVDC topologies are advantageous for the integration of power plants for renewable energy sources into AC networks with high efficiency and precise control. The characteristics of HVDC transmission system are then explained, representing the advantage of using such a system in various applications The last section deals with HVDC power cables and their properties. The current distribution and the resulting electric and magnetic fields. The case of a shared transmission tower for HVDC and HVAC lines and the electromagnetic interaction between the power lines. And finally, the main point of this work to show a method of sizing a DC power cable with highlights on the different losses that occur in the transmission DC power line. The Itaipu 6300 MW ± 600 KV project is taken as a case study.

2 Comparison of AC and DC transmission systems

Alternative Current (AC) plays a major role when it comes to industry, domestic connections and power lines over short distances. Yet, using AC systems over long distances creates several problems, on the top of these problems it has a very high investment and difficulty to control it due to frequency fluctuations. On the other hand, the use of Direct Current (DC) opens new approaches to overcome these problems arising from the use of AC systems for the transmission of high-power reaches hundreds and thousands of megawatts over long distances. Therefore, a good evaluation comparison between the two transmission systems AC and DC must be introduced to make the right choice of when it is better to install one of them or even both, taking into account various parameters such as economic or technical reasons and how to be considered efficiently and the transmission system is reliable.

2.1 An economic evaluation

There are many factors that divide the cost of a transmission line and determine the main investment for installing the infrastructure of a transmission system (i.e. towers, power cables and isolators), not to mention one main factor, the Right of Way (RoW), that relies on the peak voltage level of the line and the height of the tower, hence the section of the land which is used for the construction, maintenance and operation of the transmission system. RoW can influence on the capital investment, for instance, assuming for the same peak voltage values of an AC and DC transmission line incur the same costs for insolation. The DC line with two conductors (positive and negative polarity to earth) can carry the same power as an AC transmission line, for which three conductors of the same size are required. Therefore, a DC transmission line has the advantage of less costs for structures, insolation, number of conductors, simpler and cheaper towers. The fact that only two conductors are used in a DC line for the same current capacity as in AC lines leads to lower power losses of about two thirds compared to an AC transmission line, also to the skin effect phenomena that cannot occur in DC lines as opposed to AC lines of frequency changes can help in reducing power losses as well. The terminal equipment plays an important role in line costs, in case of DC line there is no reactive power, hence no need to install reactive power compensation as an AC line. However, the terminal equipment costs can be increased in DC line because of the necessary of using power converters and filters. From an economic standpoint, there is no doubt that the correct selection of a suitable DC or AC power line depends on the distance between the receiving and end points or source and load. Figure (1) shows the “breakeven distance” that determines whether it

is economical to establish DC or AC line, for distances smaller than the breakeven distance, AC transmission line tends to be more economically effective and beyond that it gets more expensive unlike DC line for longer distances. The breakeven distance for overhead lines varies from 400 to 700 km depending on the cost per unit line [37], and about 50 km for submarine cables [7]. In summary, the choice of using a DC transmission line can significantly reduce the long-distance capital cost.

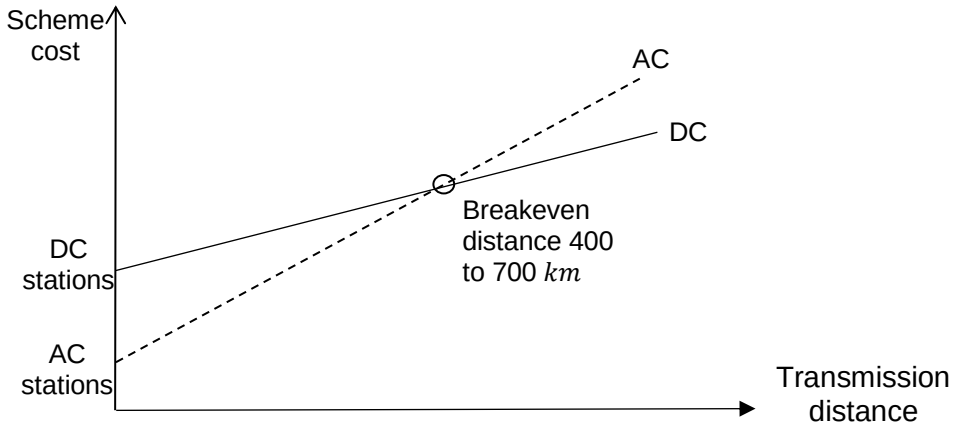

Figure (1) economic comparison of AC and DC from distance perspective [ibid.]

There are some practical projects that have been set up based on the pervious evaluation such as, in Itaipu, Brazil over 800 km distance using a High-Voltage Direct Current (HVDC) transmission system to link between 50 Hz and 60 Hz systems transmitting 6300 MW of hydropower for economic reasons. This project is considered one of the world's formidable HVDC transmission projects due its high-power rating and rated voltage of ±600 KV DC, it consists of two bipolar DC transmission lines that are able to deliver twice the rated power (12600 MW). Another project in India, Rihand-Delhi, for the transfer of around 1500 MW of thermal power to Delhi via a HVDC system, which was selected after investigations for economic reasons, lower power losses and minimal RoW instead of a 400 kV AC system [33]. According to [48] and the currency exchange rate to EUR when this work was written a cost evaluation is presented in the following a table shows an example of a comparison between two AC and DC transmission systems of the same rated power is introduced.

Table (1) cost comparison between an AC and DC transmission system [ibid.].

Parameters	Bipolar DC transmission system (+800 KV)	AC transmission system (765 KV)
Rated power (MW)	3000	3000
Costs of converter station + reactive compensation equipment (M€)	458 €	566 €
Transmission line cost (M€/mile)	1.75 €	2.52 €
Distance (miles)	1000	1000
Transmission line cost (M€)	1,750	2,520
Total cost (M€)	2,208 €	3,086 €

As can be seen in Table (1) above, the capital cost of an HVDC transmission system is lower than in the case of an HVAC system. The cost of the converter stations and the voltage level of the transmission line also contribute significantly to determining the total cost of the transmission system. The costs of a typical converter station are divided into different parts that share the total costs such as control units and filters. However, around 50% of the costs are accounted for by three components: construction 14%, converter transformers 16% and valves 20%. Added to this are the distance and the cost of the transmission line, which increase with distance. Even considering the cost of losses, life cycle and cost of interest of return which all must be taken into account for both systems, HVDC over long distances still has the advantage over HVAC [33]. Insights from the cost assessment of the Nelson River Bipole 1 HVDC transmission case study showing the installation costs of the AC transmission line and its station costs compared to the DC line and its station costs. The project was carried out in 1985 and in order to make the costs appear more realistic, a multiplication factor of 1.73 is used to convert into the present assessment. The calculations result in an estimated total cost for a 500 kV

substation and its all components from circuit breakers, power transformers, switches, control and protection units, capacitors, …etc. This total cost is approximately €16.7×10^6 for each substation at both the receiving and transmitting ends which accounts in total a cost of €33.4×10^6, while the cost for a typical 500 KV AC transmission line is considered to be €846 KV/mile and the distance of this project is 556.2 miles, making the total transmission line cost is about €235.3×10^6. Hence, when using an AC transmission system, the total cost would be around €268.7×10^6. On the other hand, in a typical HVDC system, the main components that have a high share of about 50% of the total investment are the converters and their supplements in DC stations. For the Nelson River Bipole 1 ±450 KV DC with a rated power of 1854 MW is connected to 138 KV AC at Radisson and 230 KV AC at Dorsey. The calculations for the converter stations of the DC system was done using per unit method, taking 138-230 KV as base, therefore the multiplier for 138 KV and 230 KV is 1, and for 450KV the multiplier is 1.15 and taking 1 p.u. €/KW is equal to 100 €/KW with cost range of 0.62 to 0.82 in per unit.

Table (2) estimated cost of the converter stations of 450 KV DC transmission line

Voltage level	138 KV (per unit base)	230 KV (per unit base)	450 KV
Multiplier	1	1	1.15
€/KW cost (per unit value)	$0.62 * 1.15 * 1 = 0.713$	$0.82 * 1.15 * 1 = 0.943$	Average value $\frac{0.805 + 1.0695}{2} = 0.828$
€/KW cost (actual value)	$0.713 * 100 * 1854 * 10^3 = 132.19 \times 10^6$€	$0.943 * 100 * 1854 * 10^3 = 174.83 \times 10^6$€	Average value $0.828 * 100 * 1854 * 10^3 = 153.51 \times 10^6$€

As illustrated in Table (2) above, the estimated average cost of the converter stations is about €153.51×10^6. The DC transmission line cost of ±400 and ±700 KV varies from approximately €280 to €330 KV/mile and by taking the average value for ±450 KV DC we get €305 KV/mile. Then for 556.2 miles the cost of the DC transmission line is €76.33×10^6 and by summing up both costs we get the total cost of the DC transmission system which is about €229.84×10^6. This shows a difference of €38.86 million lower in the DC transmission system than the AC one and proves that HVDC is economically superior to HVAC over long distances [23].

2.2 Technical evaluation

Proceed to the next comparison point between AC and DC transmission systems, related to some technical definitions and problems that may occur with one or both systems, and show which system has the advantage and can overcome them. In an HVDC system, it consists of many components with different objectives. The main part, however, is the power electronic devices, which are essential on the transmission and recieving side. They enable quick and high controllability at the DC cable terminals. This has the advantage on the DC line that it is more stable than on the AC line and the fault currents can also be limited more quickly in the DC line. In addition, the DC power line can overcome some of the obstacles and problems that exist on an AC power line. These problems are shown below:

2.2.1 Power capacity and losses over long distances

In an AC transmission line, the transmitted power between its terminals is inversely proportional to the distance between them. This happens because the power over an AC line is completely dependent on the angle difference between the voltage phasors, and this angle gets bigger with distance which limits the transferred power. Yet, with DC line the distance of transmission has no influence on the power capacity [37]. In addition, for an AC transmission system, the longer the transmission distance becomes, the higher the line capacity, which increases the reactive power. A matter that limits the use of long-distance AC transmission lines. On the other hand, there is no reactive power for DC lines, making HVDC more applicable for transmitting large power between two points for long distances. The losses in an HVDC transmission system come from the converter stations where each station counts with 0.6% of the transmitted power plus the losses in the transmission line, for the same power capacity the HVDC transmission system still has lower losses in total compared to an AC system [7].

2.2.2 Voltage control complexity

The voltage control process in an AC line is more complicated and depends on the Surge Impedance Loading (SIL), due to voltage drop which might happens because of excessive loads (i.e. extra connections or high resistance components). In normal operation, the voltage profile is the same for a transmitted power in terms of its SIL when both receiving and sending voltages are equal at the line terminals [37]. The Surge Impedance Loading is referred to as the natural load of transmission line where the voltage and current are in phase across the entire transmission line, and the load at which the reactive and inductive power are opposite and equal

is called surge impedance load. The main parameters along a transmission line are the capacitance which feeds reactive power to the line and inductance that absorbs the reactive power. For a compensation operation in which both capacitive and inductive powers are the same, we get:

$$Z_s = \sqrt{\frac{L}{C}}$$

Where L: the inductance per unit length of the line

C: the capacitance per unit length of the line

Z_s: the surge impedance

The surge impedance of a transmission line (Z_s) can therefore be regarded as a pure resistance which if it is connected to the receiving end of a line, the reactive power all over this line is totally absorbed by its inductive reactance. Therefore, the Surge Impedance Loading (SIL) is defined as a power transmitted over a line to a purely resistive load, the value of which is equal to the surge impedance of this line [10]. When the voltage drop occurs, the voltage profile changes with the line loading, for higher line loading than SIL and in order to keep the voltages at the line ends fixed, the midpoint voltage is reduced and increased in case of loadings less than SIL. For a constant voltage at the receiving and sending end, reactive power control is required when the line loading changes, and as the length of the line increases, further maintenance configurations are needed. In contrast, DC lines are not affected and do not require any reactive power control. Although reactive power corresponding to the transmitted power is required at the DC converter stations located at the end of DC lines, the lines themselves are not influenced by any generated reactive power [37].

2.2.3 Stability

With different AC networks, it is sometimes impossible to synchronize between two due to frequency differences (50 and 60 Hz), long distances and stability problems. Replacing AC transmission lines with DC lines is the only solution to connect two networks with different nominal frequencies as in Japan and South America. Furthermore, the DC interconnection link does not participate with increasing short circuit fault current if it happens on the AC side [7]. In Japan, half of the country relies on an AC network with 60 Hz frequency and the other half uses 50 Hz system. Although the distance between them is not long enough to link them with a DC connection, it is still impossible to link them with a direct AC interconnection and the only way

for transferring power between them, is to set up two converter stations at the end of each network and connect them with a DC link, the two AC networks stay connected as well [41].

Even though when two AC systems tend to be coordinated by using some controller devices for line power and frequency signals, still the interconnection between them might pose some problems, such as, large power oscillations and disturbances in the system that can be transmitted from a network to another. On the other hand, if the linkage is done by using DC line, these problems do not arise thanks to fast switching and controllability in the DC converter station. Moreover, when using an AC line for long distance, the line itself should be compensated using series capacitors, shunt inductors and Static Var Compensators (SVCs) that can control and maintain transmitted power and peak voltage to overcome stability constraints[37]. The SVCs are electrical devices that are used for regulating bus voltage in the AC transmission line constantly to cope with the fluctuations in the reactive power loading. They mainly consist of a fixed capacitor that works alongside a thyristor-controlled reactor [34].

2.2.4 Existence of ground current

Ground impedance is considered to be a major problem in the AC system in the event of ground current being present. This leads to unbalanced operation, inefficient power flow and can cause some telephonic interference. Yet, the ground impedance has no influence on the DC link. In fact, in a single-pole (monopolar) operation where only one conductor supplies power, grounding acts as a return line. For such a system, it is only uncomfortable if some metals are present and suffer corrosion from DC current flow. Therefore, it is possible to operate a DC system with ground as a return, as opposed to an AC system for unbalanced operation, which can cause many problems and disturbances that are unacceptable [37].

2.3 Environmental impact

HVDC has smaller right-of-way than an AC system of the same size, hence it has less effect on the environment and requires less land to cover the overhead transmission lines. For the existing RoW of an AC system. The existing RoW of an AC system can be used to provide more power when replaced by a DC system. In general, the HVDC system is more compatible with the environment from the point of view of visual impact. However, HVDC has some demerits such as, it requires extra space for the power electronic devices and the converter stations that can lead to radio interference, perceptible noise and electromagnetic fields[7]. The transmission system function is to deliver power from the generation point to the consumers (e.g. residential, industrial or rural areas …), for high demand or interconnections using HVDC system, the

transmission lines might carry power in hundreds or thousands of Megawatts (MWs) and have typical voltage of 400-1000 KV. These transmission lines are routed through nature (for instance, land, desert, forests, water, mountains and some inhabited areas). For this reason, the effects of ultra-high voltage transmission lines must be carefully analyzed to examine their effects on the environment and on people[41]. These effects are commonly represented in magnetic fields, corona phenomena, electric fields, acoustic noise, radio interference which are explained in the following:

2.3.1 Magnetic fields

When current flows through a conductor, it creates a magnetic flux which is several magnetic lines that pass through a surface. The direction of the magnetic field depends on the direction of the flowing current and its amplitude on the distance from this conductor and the amplitude of the current as well. For a HVDC transmission line of ± 450 KV, it can produce a magnetic field with density of about 25 μT (micro-Tesla), where the earth itself has a natural and permanent magnetic field of 40 μT [36]-[41]. The magnetic field value is directly proportional to the magnitude of the current and inversely with the distance from the conductor [36] as shown in the following formula:

$$B = \frac{\mu_{\circ} I}{2\pi r}$$

Where B: magnetic field magnitude (Tesla, T)
$\mu_{\circ}$: permeability of free space ($4\pi * 10^{-7} T.m/A$)
I: magnitude of the electric current (Amperes, A)
r: distance from the conductor (meters, m)

2.3.2 Corona Phenomena

Corona phenomena happens on the surface of high-voltage overhead transmission lines and its effects must be studied well for designing and constructing a transmission system, its main effects are corona loss (power loss), radio interference and audible noise. It occurs when the medium which is air and exists between the conductors breaks down due to high voltage potential which creates electric field, with the help of foul weather conditions (i.e. fog, water drops, snow, etc.), or because of some impurities on the surface of transmission lines such as conductor nicks, or cracks, some airborne dust and insects, under these circumstances and if the electric field intensity reaches beyond the air breakdown strength limit which is about 30 KV/cm under standard temperature and pressure levels, corona discharge starts and this

results in ozone production, noises, radio frequency disturbances, glow light and conductor vibration [40]. Corona charge participates with a small portion in ozone production in the environment, the natural concentration of ozone in the atmosphere is almost 50 ppb (parts per billion) and in the city it reaches to 150 ppb. However, corona increases the ozone production for both AC and DC lines with small values around 10 ppb, it is still down the critical risk values that fall between 180-200 ppb [41]. In the case of corona loss in HVDC, this is a consequence of the space charge and therefore mainly depends on the pole space, although with an increase in the voltage, which gives the same value of the corona loss as the space charge, the pole spacing still has the greatest influence on the corona loss. On the other hand, in AC transmission lines corona loss relies on the conductor dimensions and corona-free surface gradient, this means that any change occurs on the surface gradient has the same corona loss value as a result of voltage change or phase spacing. With audible noises, the levels in both systems differ depending on the weather conditions, with dry and fair weather the audible noises are higher with HVDC and higher with AC lines in wet weather conditions. If the corona phenomena occurs in HVDC under wet weather conditions, this leads to a high space charge around the conductor, which reduces both the electrical field on the conductor surface and the intensity of the corona current. This helps reduce audible noise in wet weather than in dry weather. Like audible noise effect, the Radio Interference (RI) has higher levels for HVDC in dry weather, and on the other side, under wet weather conditions AC line has the highest levels. RI which is known also as radio noise refers to any unwanted interference in a transmitted radio signal from any device, for instance, due to the presence of electric waves that can interrupt it. When corona charge takes place in wet weather, waterdrops that are present on the conductor surface due to their shape, they have onset corona electric fields which are different and lower than the conductor electric field itself, in case of HVDC, an almost uniform ion cloud is formed around the DC conductor due to the high intensity of space charge and air ionization, which works on maintaining the surface conductor electric field to the waterdrops onset corona field. On the contrary, because of the nature of AC transmission lines electric field that prevents any formation of a uniform ion cloud of the same polarity, as a result of that the RI has the highest level in wet weather in AC lines than HVDC lines [40].

2.3.3 Electric field

There is always a magnetic field around power lines that carry high currents, which is measured in milliGauss (mG) and an electrical field in KV/m, the electric field can be shielded by fences, concrete, buildings, etc. The electric field is generated because of the potential difference

between the conductors and each other or the earth or space charge due to corona. These fields can produce static charges by capacitive coupling with conducting objects and circulating currents through inductive coupling, many studies agree on that the micro induced flow currents through the human body over time cause serious health problems according to the exposure time and the strength of the field. The electric field is a vector quantity that means it has a direction and magnitude and its magnitude mainly dependent on the magnitude of the conductor voltage, higher voltages the electric field intensity increases. Besides, some other factors play a role in electric and magnetic fields production such as, the height of the conductor to the ground, the radius of the conductors, phase symmetry and the position of the conductors with respect to each other or the measuring devices[47]. The strength of electric field has the highest value directly under the transmission line, for ± 450 KV line it has a value of about 20 KV/m and this value changes according to the weather conditions and humidity in the atmosphere. DC transmission line has less problems related to electric field than AC system, thanks to the steady-state process in HVDC, less need of Right of Way (RoW) and lower heights for the supporting towers [41].

2.3.4 Acoustic noise

Among all sources of audible noises that come from railway roads, traffic, factories, etc. There is still a small part caused by the transmission line systems and the main source of it the transformer station. For HVDC transmission line system, although it consists of different components that can make noises, the loudest noise comes from the transformer which is dependent on the core flux density. All noises come from HVDC system including converter transformers and operational process make noise of 10 dB higher than that of no load operational with frequency ranges between 300 to 3000 Hz, where no load operation makes noise of 10 to 20 dB higher than full load operation. Yet, these noises can be reduced by well-made shielding, more efficient equipment or separate noisy low-quality equipment with distance. The HVDC transmission system produces noise at a distance of 350 meters of less than 10 dB and is generally better than the HVAC in terms of visual impact [41].

2.3.5 Radio Interference (RI)

The main reason for radio interference in HVDC is the switching process in the converter stations through thyristor valves and other power electronic devices that work in fast sequence under high power ratings, resulting in harmonic waves in kilohertz or megahertz due to voltage changes, fast current variations. These harmonics oscillate to the transmission lines and cause

potentials that interfere with telecommunication signals whose frequencies fall in the harmonics-frequency region. The RI levels diminish with the distance from the conductor, they are lower in HVDC than in HVAC, for example, for 300 meters away from a DC line it has RI level of 40 dB (Decibel) comes from frequency of 0.5 MHz and for 380 KV HVAC transmission line has a value of 50 dB. The use of suitable filters can help to reduce radio interference to a minimum [41].

3 HVDC transmission system

The main goal of a power transmission line is to transmit a large amount of power from the generating station to the consumers, and it is either an AC transmission system or a DC transmission system. The world's most widely used electrical energy transmission system is the AC transmission system. The High-Voltage Direct Current (HVDC) transmission system is the best solution when it comes to providing large amounts of energy (megawatts). It has been shown that over time with a capacity of up to 100 gigawatts (GWs) until 2010 after the first installation of the HVDC transmission system in 1954 [29]. HVDC system is used for transmitting bulk power in point-to-point configurations. The DC line is linked to a synchronous AC source through power electronic converters that converts AC current into smooth DC current with the help of proper filters [7]. The two available used technologies for HVDC transmission systems are based on the type of source converters, which are voltage source and current source converters. The Voltage Source Converter (VSC) relies on the function of Insulated Gate Bipolar Transistors (IGBTs), while the Current Source Converter (CSC) which is named also as Line Commutated Converter (LCC) deals with high power thyristors after using mercury valves at first [29].

3.1 Current source converter HVDC system

The current source converter was the first technology to use for implementing HVDC system and its performance depends on the switching process of the thyristors. The CSC principle is to work as a reactive power compensation and on filtering the generated power wave after conversion [29]. The used thyristors are four-layer silicon semiconductor devices that are switched on or off by applying a gate pulse for the on-state and removing the gate current for the off-state. It is used for transmitting bulk power of up to 6500 MW for each single overhead HVDC line in a point-to-point transmission link and has a wide range of DC voltage ratings till ±800 KV. Moreover, the ability of high current ratings of up to 6250 KA and blocking voltage up to 10 KV, Making this type has the highest power and voltage ratings among HVDC converter

technologies [25]-[42]. The CSC has many advantages that give it the priority to be widely used. It is available for high power and voltage ratings, low losses thanks to the thyristors during the switching process when they switch off, the current through them drops to zero and the thyristors themselves can withstand sudden high transients of loads. However, CSC has some drawbacks as well, it can suffer from commutation failure as for both sides at the end of DC link the used rectifier and inverter get their inputs from the AC synchronous network and draw reactive power from it, when voltage drop happens on the AC side, the valves might not working properly or stop and cause commutation failure. Furthermore, complexity in the filtering process due to large harmonics from the AC current, they can be reduced by using 12 or 24 pulse converter bridges, yet it depends on the performance and the transmitted power ratings, it requires large harmonic filters and these filters can provide some reactive power as well [42]. The controllability of thyristor switching during turn-off process might cause some problems during operation of CSC, as it leads to poor power factor and waveform distortion [29]. The CSC system is characterized by a constant unidirectional output current and is therefore referred to as a line-commutated converter. This is accomplished by controlling the firing angle (α) of each rectifier and inverter. When it is desired to reverse power from one station to another, the voltage polarity of both stations is inverted, but the current direction is kept the same and fed to the AC side. The operation of this technology is classified with low maintenance, high reliability and robustness. Therefore, it is preferable to use in most HVDC transmission projects [25]. The CSC-based HVDC system consists of two thyristor converter sets at each end connected to AC networks through a star-star (YY) and a star-delta (Y-Δ) connections with the transformer, where the high voltage side is connected through a grounded star configuration and the low voltage side in a delta arrangement. This kind of connection is to control the phase-shift angle between the two voltage sets and ensure a phase-shift of 30º between them, thereby boosting the voltage sets of the generators. The two-thyristor converter sets on both sides are linked together with a positive and a negative pole with respect to ground as shown in Figure (2), and through a series connection for some inductors that help to keep the DC current robust and increase the reliability of the system [24]. Many CSC-based HVDC systems have been implemented in different countries to transmit bulk power over long distances. For example, in 2013 the Rio Madeira project was carried out in Brazil to transmit 6300 MW over 2375 km with a rating voltage of ± 600 kV. In India, a Biswanath-Agra project was accomplished in 2014, which crossed 1728 km to deliver power reaches 6000 MW at a voltage rating of voltage of ± 800 k. Another project was implemented in 2011 between UK and Netherlands with a power capacity of 1000 MW at ±400 KV over 260 km. As well, in China several projects have been taken place

for this type of HVDC technologies, the Zhundong-Sichuan project in 2015 which is at the top place among these projects in China by having the highest transmitted power of 10000 MW at rated voltage of ±1100 KV and over the longest distance 2600 Km [25].

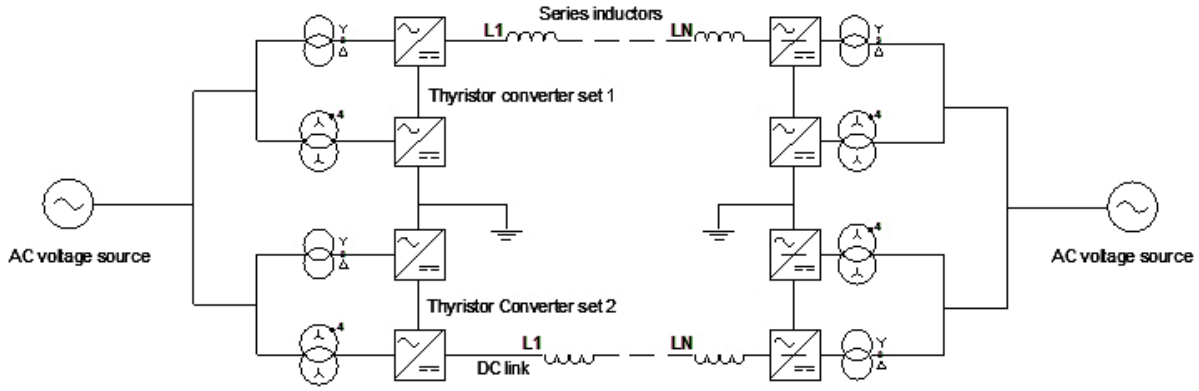

Figure (2) block diagram of current-link converter HVDC system [24].

3.2 Voltage source converter HVDC system

HVDC transmission systems based on voltage source converter technology rely on the use of IGBT (insulated gate bipolar transistor) devices for switching process, in which the current can be switched on or off at any time regardless of the AC voltage. High frequency pulse width modulation technique is used to control the performance of the converters and keep the output voltage constant. Besides, these converters are designed so that they are well qualified for controlling their active and reactive power. Due to the use of the pulse width modulation method to reduce the converter harmonics and switching IGBTs on and off frequently in one cycle, the switching losses are high and the converter overall performance suffers from a low efficiency comparing to CSC-based HVDC. This happens when a two-level voltage source converter is in operation, thereby to overcome this poor efficiency a three-level or multi-level converter is installed [25]. Voltage source converter can overcome some problems that exist in current source converter which requires reactive power support from the AC source, whereas VSC can operate at any active and reactive power and support reactive power to each converter. This counts as one advantage of using VSC in HVDC systems. Moreover, in some cases filtering process can be removed as VSC-based HVDC can produce very good sine waveforms and

show very low harmonics, such a system has a small footprint which makes it suitable for implementing on offshore connections, beside fast installation and testing of the converter stations because of the capability of moving them fully assembled to the placement site and the ability to provide multi-terminal HVDC grids [29]. VSC-based HVDC can be installed for weak grids and as a black-start supporter in AC networks, provide high and fast controllability level and can keep constant the voltage polarity constant. Although the VSC has many advantages, it still suffers from several setbacks that limit its availability to use. It has high power losses, high costs and can be used for lower power ratings comparing to CSC-based HVDC system [42]. A basic VSC-HVDC system comprises of two converter stations which are linked through a DC link with parallel capacitors working as voltage ports to reduce voltage ripples, for this, the converters of this system are named voltage source converters as represented in Figure (3). Each converter is able to absorb or supply reactive power independently. On one side where the generated power needs to be transmitted, the AC source is connected in three-phase configurations with a transformer then linked to the converter station through an inductance and transmit bulk power over the DC link between the two converter stations. At the receiving point, the second converter is linked to an AC network through a transformer and a small inductance that might be the internal inductance of the utility system [24]. The operation of a basic two-level VSC is controlled by its switching devices by turning one device on while the other remains turned off. Simultaneous operation leads to a short-circuit failure via the capacitor, which is connected to the DC link, and thus damage the converter switches. Therefore, only one switch has to work at a time to avoid overcurrent. By turning the switches on and off in this way, two complementary voltage values ($+\frac{V_{DC}}{2}$ and $-\frac{V_{DC}}{2}$) are generated at the converter AC output terminal. The VSC is characterized by flexibility in operation, which makes it suitable for urban areas and can be installed for applications with a rated power of up to 1800 MW. For example, A Nordlink 1400 MW, ±525 KV project was carried out to interconnect two networks between Germany and Norway over 623 Km using VSC-based HVDC technology. In 2009, a Borwin 1 project was implemented in Germany with a distance of 200 km, providing a capacity of 400 MW at a rated voltage of ±150 kV. In 2013, another scheme for the delivery of up to 1000 MW over 65 Km was installed in France. In Norway, a Skagerrrak4 700 MW, ±500 KV project was undertaken in 2014 crossing a distance of 244 Km [25].

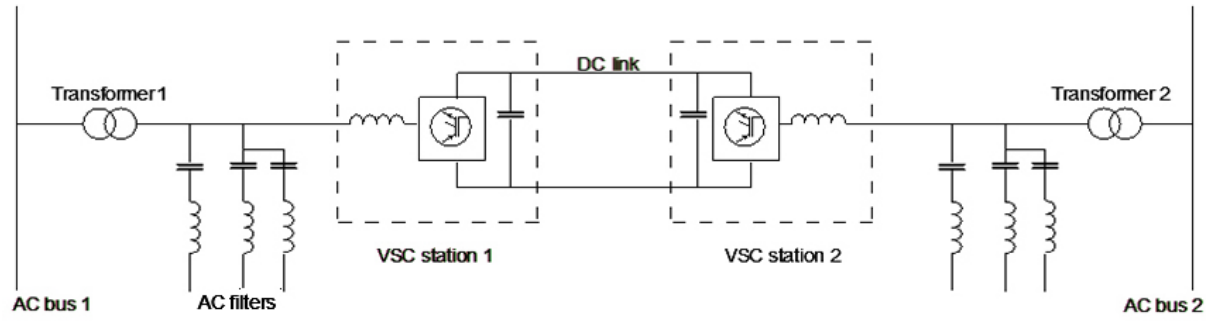

Figure (3) block diagram of voltage source converter HVDC system [24]

3.3 Comparison between VSC-HVDC and CSC-HVDC

Both systems are explained as already mentioned. The following Table (3) provides a good comparison to assess, clarify and summarize the conclusion between the two systems in terms of many differences such as the used technology, switching conditions, filtration process for AC and DC harmonics, voltage and power ratings, type of grid connection, problems that might occur while in operation and others.

Table (3) a comparison between VSC-HVDC and CSC-HVDC [25].

Differences	VSC-based HVDC	CSC-based HVDC
Used technology	Depends on IGBT devices technology.	Uses thyristor-based devices.
Power and overload capacity	Supports low power capacity and has a weak overload ability.	Can support high power and a good overload capacity.
Switching conditions	The switching process for both cases, in which IGBTs are switched on or off, takes place via an external circuit.	In the case of switching on, this is done by applying a gate pulse and switching off with the help of an external circuit.
Operation performance	The current direction changes with power.	Current flows in one direction.

	Changing the current direction reverses the power. Capacitive energy storage. Uses conventional transformers. Has a built-in black start technique. Characterized by a good control of the reactive power.	Power can be reversed by inverting the voltage polarity. Inductive energy storage. Needs converter transformers. Requires an external unit to perform black start operation. It has a poor control of reactive power.
Applications	Used to transmit power from remote areas generated by renewable energy resources. Operating voltages up to about 600 KV. Suitable for connection to weak AC networks where good performance can be achieved.	It is mainly used to transmit enormous power over long distances. Operating voltages up to over 1000 KV. Requires a strong AC grid to keep performance high and efficient.
Losses and harmonics filtration	higher losses. It generates low harmonic levels and therefore does not require filters.	Lower losses. AC and DC filters are required to cancel harmonics.
Environmental impact	It has a better visual impact and more compact area.	Requires larger area due to harmonic filters.
problems	Thanks to the flexibility of the switching process, it can withstand voltage drops from the AC voltage. Therefore, there are no problems related to commutation errors and this	Can be affected by voltage drops or phase shift fluctuations in the AC voltage that result in a DC transient overcurrent and a commutation failure. This effect is taking place within a few power

	makes it practical for multi-terminal HVDC connections that support multiple independent power flows. Turning off the IGBTs alone cannot prevent or stop short circuit failure on the DC line, due to the presence of the diode and its continuous conduction, which will increase the DC fault current. Opening the circuit breakers at each end of the transmission system is the only solution to remove the fault and diode conduction.	frequency cycles. Due to commutation failure that can happen when set the converter from rectifier mode into an inverter, thereby CSC-HVDC is not practical to be used in multi-terminal HVDC systems. If a short circuit fault occurs on the DC line, this can be dissipated by controlling the firing angle of the thyristor valves, which reduce the short circuit effect.

4 Components of a HVDC transmission system

The HVDC transmission network consists of various parts that are combined to build the system. The most important parts among them are mainly divided into two sections, namely the converter station and the transmission medium, which are explained below.

4.1 Converter station

The converter station is a substation where all power electronic devices, converting units, filters and other circuit components such as, levelling reactors, capacitors, inductors, etc. are placed. It includes the converter transformer, which is arranged in two windings, one with the AC side winding and the other with the valve side winding. The converting station mechanism is to be able to convert from AC to DC and the other way around, when converting from AC to DC, the process is called rectifier and the inverter when converting from a DC input to an AC output. Each station should be designed to work in both modes (rectifier and inverter). In addition, some other devices are required amid converter stations as a source for reactive power because the operation of converters requires reactive power which can be supplied from static VARs or shunt capacitors. Filters that are necessary at each station in order to eliminate harmonics and

smooth the output waveforms, the filtering process consists of different types of filters made of AC filters, DC filters and some filters for high frequencies to avoid radio interference [17].

4.1.1 Six-pulse bridge converter

As mentioned above, the converting units are the rectifier and inverter converting units where they convert from AC to DC and vise-versa. This is done by using a six-pulse modulation in three-phase bridge converter configurations, this circuit is known as Graetz circuit. In some cases of HVDC systems, two six-pulse bridge modulations are connected to obtain a twelve-pulse bridge converter [17]. The main part of the converting unit is the valve or valve arm, it can be either non-controllable or controllable valve. When one or two power diodes in series are used, it is non-controllable valve and controllable when it is built up from one thyristor or more in series. The six-pulse bridge converter is described as a double-way connection where six valves are connected with a three-phase AC supply through its converter transformer in star-star (Y-Y) arrangements as shown in Figure (4-a) and has a block diagram symbol of Figure (4-b) [8].

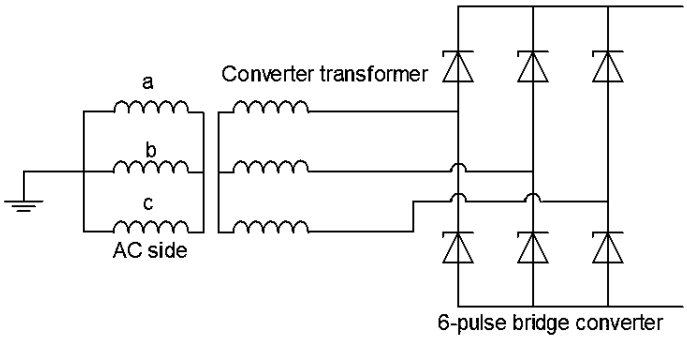

Figure (4-a) six-pulse bridge converter unit [ibid.].

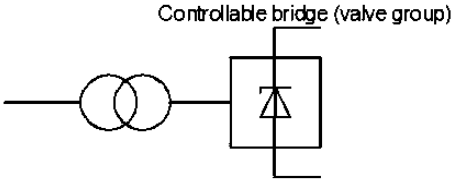

Figure (4-b) block diagram symbol of six-pulse converter unit [ibid.].

The six-pulse converter generates current harmonics of the order 6n±1 on the AC side and DC voltage harmonics of the order 6n on the DC side where n is for all positive integer numbers. Tuning is required to deal with 5^{th} and 7^{th} harmonics, alongside with the help of DC reactors and surge arresters to ensure reliability of the system with no disappointments. DC reactors are connected to each pole of the converter station and their functions are smoothing the DC current and reducing harmonics to keep a continuous operation, as the rate of change in DC and the commutation processes of converters are controlled by DC reactors [8]. Furthermore,

they help to facilitate any expansion that might exists in the direct current, minimize any steepness or surges of voltage and current on the DC line and provide compensations when needed for any defect in inverter process [17]. Surge arrestors are mainly used to protect the equipment of over-voltages failure regardless of their sources. They are connected across every valve in the converter unit and across each converter bridge as well [8].

4.1.2 Twelve-pulse bridge converter

Figure (5-a) shows a construction of twelve pulse valve groups, in which two converter transformers are used to allow power flow between AC side and DC side. The 12-pulse bridge converter is used in modern HVDC and each valve group is constructed using thyristors connected in series, the number of the used thyristors depend on the voltage rating across the valve terminals [17]. This configuration is almost used in every HVDC power converter, the DC side is connected with the two transformers once in an underground star-star connection and the other one in a star-delta connection. The twelve valve groups are connected in such arrangements so that the applied voltage on each six valve groups cause a phase shift of 30º, which helps to cancel the 5^{th} and 7^{th} harmonic currents on the AC side and the 6^{th} harmonic voltage on the DC side, that can share in a significant reduction of harmonic filters. The twelve-pulse power converter has three quadrivalve groups as shown in Figure (5-b), each one of them includes four vertical valve groups assembled as one valve and structured from hundreds of thyristors connected in series for high voltage ratings in several KV and has a long mechanically structure that allows it to be hanged from the valve hall as all thyristor converters are placed in one hall called the valve hall, while the converter transformers are sited in the switchyard. These transformers work on adjusting the AC voltage to the suitable operating voltage for DC system and feed the bridge valves with the right voltage. Figure (5-b) demonstrates the block diagram of a twelve-pulse converter [8]. On the AC side, the twelve-pulse converter produces current harmonics with characteristics of the order $12n\pm1$, whereas voltage harmonics on the DC side have the order of $6n$, therefore harmonic filters are required on both sides. For a twelve-pulse converter, AC filters are usually set to 11^{th}, 13^{th}, 23^{rd} and 25^{th} harmonics and they can be switched using circuit breakers or switches to control the reactive power since these filters are able to generate reactive power at the fundamental frequency. On the DC side, the DC filters work on smoothing the DC current flow and eliminate any harmonics on the transmission line, hence reducing the possibility of frequency interference with communication signals and minimizing coupling [8].

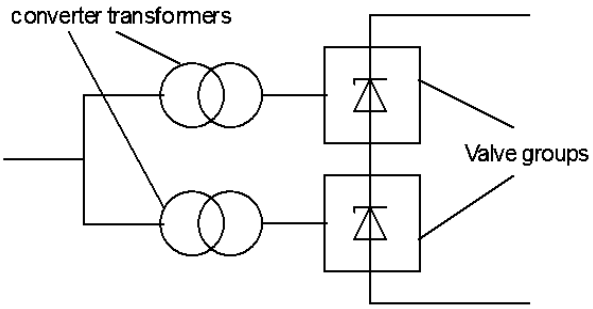

Figure (5-b) block diagram symbol of a twelve-pulse bridge converter [ibid.].

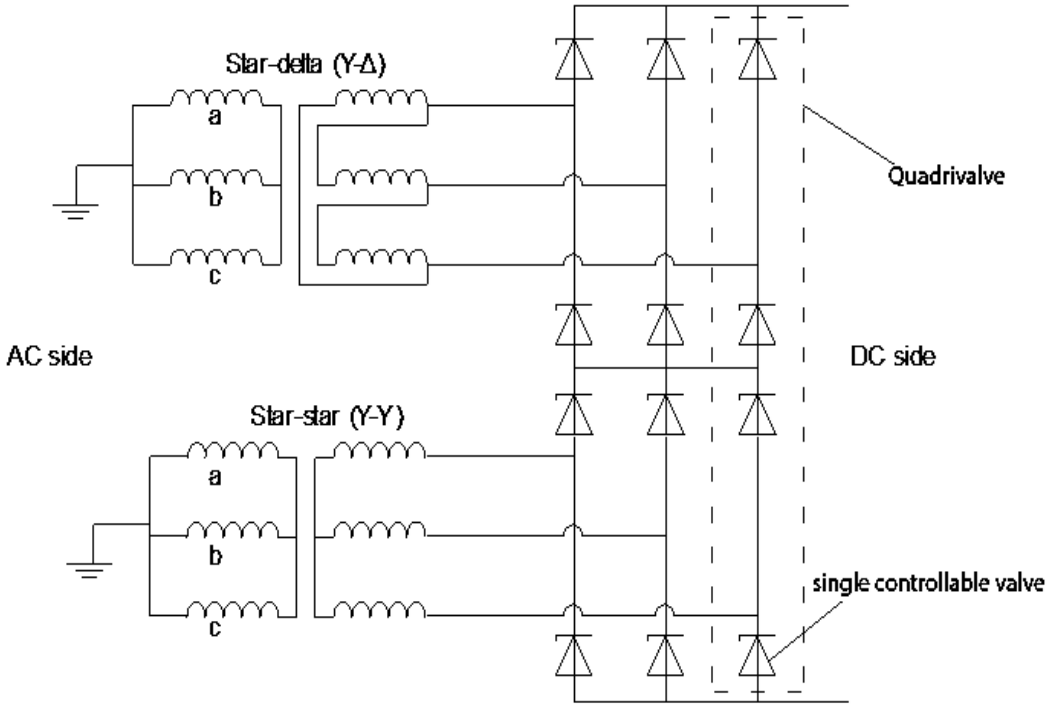

Figure (5-b) twelve-pulse bridge converter modulation [17].

4.1.3 24-pulse converter

In HVDC systems, in particular in VSC-based HVDC systems, in which PWM control (Pulse Width Modulation) is used and which are generally constructed in two-stage configurations, yet the PWM method has a major problem that the Switching losses increase with the switching frequency. Therefore, multi-pulse converters are used as an efficient alternative method to eliminate lower order harmonics and reduce higher order harmonics in HVDC transmission systems to reasonable values. The percentage of Total Harmonic Distortion (% THD) is defined

as measuring the harmonics present in a generated waveform. In the case of two-stage multi-pulse converters, the %THD of their stepping voltages vary with the number of applied pulses and is characterized in that it decreases by increasing the pulse number, for a six-pulse converter is measured as 30.9% and for 24-pulse converter is 7.5%. Nevertheless, this value of 7.5% THD is still greater than the specified by IEEE standard value of 5%, and to overcome that three-stage converter bridges instead of the two-stage configurations are used [20]. The 24-pulse converter can be structured using four sets of six-pulse converters connected in series on the primary side of the three-phase transformer of each set. The converter transformer is considered the main component that plays a significant role in shaping the waveform of the output voltage of a multi-pulse conversion process. One the secondary side, the windings of two converter transformers are in delta (Δ) connection and the other two have their windings in an ungrounded Wye (Y) connection. This type of connection is chosen to make it simple and efficient since it can help to radically reduce the voltage harmonics of the order 11^{th} and 13^{th}. For each set of the six-pulse converters, the phase and line voltage waveforms can be obtained by switching on each GTO (Gate Turn-Off thyristor) valve for 180º and with a pulse shift angel 120º between each phase. The operation of the six-pulse converter does not require a reactive power source like capacitor banks, but it differs when connecting the equipment with an AC bus. When the output voltage of the 24-pulse converter is not in phase with the AC bus voltage and is larger than it, the device will continue as a capacitor when a leading reactive power from the AC bus is withdrawn. When the 24-pulse voltage is less than the AC bus voltage, the drawn current is a lagging inductive current [1]. Therefore, the main objective of the multi-pulse converter controller which consists of two controllers, the DC voltage controller and the current controller, is that both controllers should be able to preserve the value of DC voltage at a specified reference value and keep the active power flow under control between the AC grid and DC side, besides compensating required reactive power to the AC mains as well. This is done with the help of a capacitor bank on the DC bus in order to keep the DC voltage at a certain value, whereby a balance of the real power between the AC and DC side is achieved [20].

4.2 The transmission medium

The transmission medium is the DC link that carries bulk power between two points. The HVDC transmission lines can be constructed as overhead transmission lines or submarine cables. The DC links are divided into three types:

4.2.1 Monopolar DC link

This type has only one conductor and uses the ground and/or the sea as a return. Therefore it is mostly used in submarine cable connections and usually operated with negative polarity due to corona effects which are less in negative polarity of the conductor than it is with positive polarity [37]. The simplest and least expensive application for this type is a monopolar system with ground return, as represented in Figure (6-a), since it requires only two converters and one conductor. It is used to transmit moderate power and commonly applied for systems where submarine cables are used as sea electrodes for return current. In some cases where such connection is not available, for instance, area with high natural earth resistivity, then a metallic low voltage cable is used as the return carrier cable for current with a simple local ground reference [3]. In addition, a metallic neutral cable is preferable to be used for cases where corrosion or harmonic disturbances are likely to occur [37].

4.2.2 Bipolar DC link

Figure (6-b) shows the construction of a bipolar DC link, in which two conductor lines with two opposite polarities are used. On the transmitting and receiving sides there are two converter sets of the same nominal ratings in series and the junction point between them is grounded. There is zero ground current flow during normal balanced operation, as both poles carry the same current value. A monopolar system can be considered as a first stage of a bipolar system, therefore, If the converter process fails, one DC cable can be used temporarily as a metallic return cable with the help of a suitable switch [37]. This type is widely-used with twelve-pulse converters, connected individually with each pole, which divides the system into two independent capable DC circuits of half capacity severally [3]. Furthermore, more than two converter sets can be installed for multi-terminal connection, in which each converter is able to work as rectifier or inverter independently [25].

4.2.3 Homopolar DC link

This type is similar to bipolar DC link, but the main difference is that the two conductors operate with the same polarity (usually negative) and it can work with a metallic or ground return as shown in Figure (6-c). The connection is made in negative polarity to minimize the effects of corona and reactive power losses and it can work as a monopolar DC link when fault occurs on one pole [25]. This system is distinguished by giving some reduction of insulation costs, but it is rarely used due to using earth return which has consequent various problems [37].

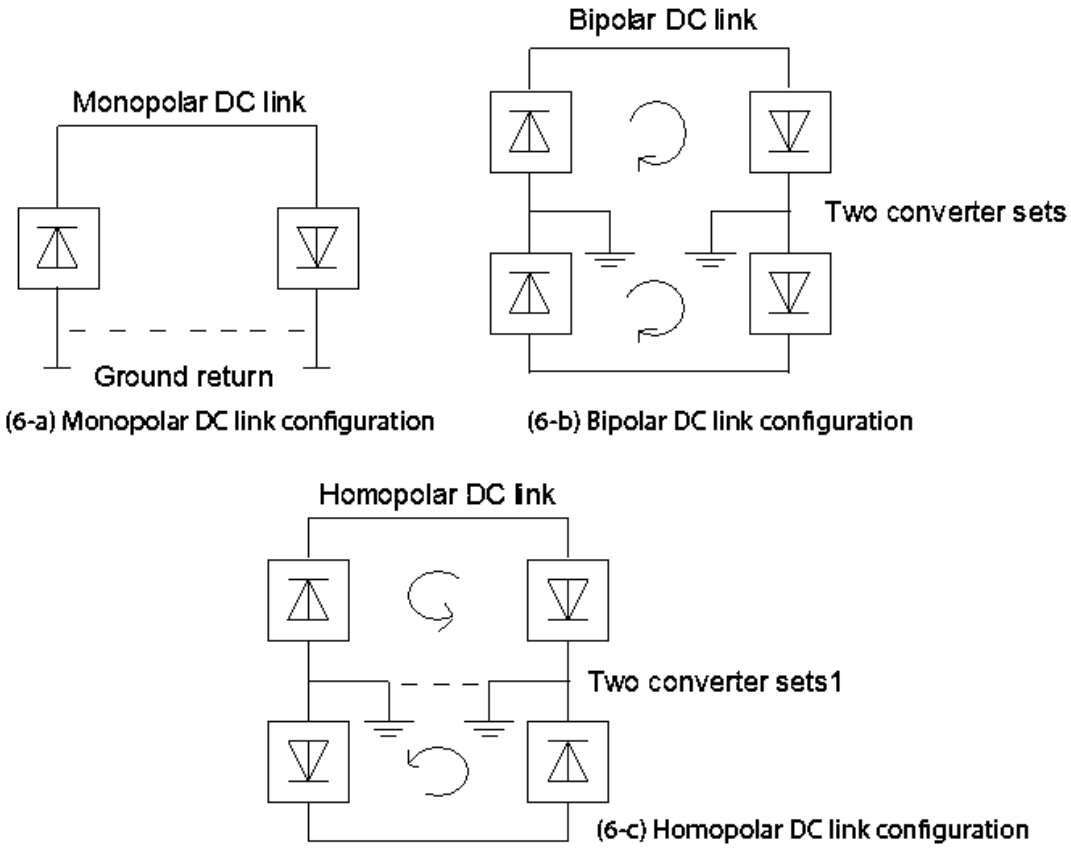

Figure (6) types of DC transmission links [37].

5 High-power semiconductor devices

The high-power semiconductor devices are the key for a reliable and robust HVDC transmission system. They have been developed to withstand higher voltage and current ratings, reduce power losses, provide high frequency switching controllability. The high-power semiconductors that used in power converters are defined based on their switching devices, they are either thyristor or transistor-based devices. Earlier used semiconductor devices are Silicon-Controlled Rectifier (SCR), Gate Turn-off thyristor (GTO) and Gate Commuted Thyristor (GCT), then with development to handle high power ratings, other power semiconductor devices are introduced such as, Insulated Gate Bipolar Transistor (IGBT) and Injection-Enhanced Gate Transistor (IEGT). Table (4) shows the voltage and current ratings for each type of these high-power semiconductor devices, each device has different specifications and range of voltage and current ratings regarding the manufacturer. For example, a SCR device manufactured by

Mitsubishi has a voltage rating of 12 KV and current ratings of 1.5 KV, whereas an ABB of the same type offers voltage and current ratings of 6.5 KV and 4.2 KA respectively [44]. The power semiconductor devices can be used for different applications that deal with high levels of power and frequencies, where the relation between power and frequency is inversely proportional to each other. Thyristors are suitable for high power and low frequency applications, nowadays thyristors are available to operate on high voltage and current ratings individually. That is why power thyristor-based devices are favored for applications such as HVDC transmission systems, just by using a single monolithic device gives a control of power up to 10 megawatts. Whilst IGBT and Metal-Oxide-Semiconductor Field-Effect Transistor (MOSFET) work as the best solutions for moderate and lower power and frequency applications respectively [5].

Table (4) voltage and current ratings range of high-power semiconductor devices [44] .

High-power Semiconductor Device	Voltage ratings range (KV)	Current ratings range (KA)
SCR	(4.8 - 12)	(1.5-5)
GTO/GCT	(6 – 6.5)	(1.5 – 6)
IEGT	(4.5 – 6.5)	(0.6 – 1.5)
IGBT	(1.7 – 6.5)	(0.6 – 3.6)

In the following the main high-power semiconductor devices that are used as components in HVDC transmission system are illustrated based on their construction, process and purpose.

5.1 Power diodes

Diodes are split up into two main types for high power applications. Firstly, the rectifier diodes which are used for line-frequency of 50 Hz or 60 Hz grids and share with power losses during the switching process. Secondly, fast recovery diodes that can work as freewheeling diodes or operate at high switching frequency, therefore they are connected usually in a rectifier output after a high-frequency transformer. The most power diodes are pin-diodes, whose middle regions are doped with lower concentration than p and n layers and have the advantage of

blocking bulk voltages due to their very reduced on-resistance after a high-level injection in the base region. Mostly these diodes are constructed of $p^+n^-n^+$ layers, and the middle layer (n^-) is specified as “i”-layer, hence this type of diodes is named pin-diodes. Diode’s function is to allow current flow in one direction which is called forward direction and block it in the opposite direction that is known as reverse direction. This performance of diode is represented by its I-V characteristic, which is defined with different parameters show the specifications of each diode. For both forward and reverse directions, these parameters have different scales and definitions. During forward bias, it is characterized by several factors which are forward current (I_F), voltage drop (V_F) and the maximum allowed voltage drop in forward direction of diode that named under the maximum voltage drop (V_{Fmax}), all values of them are approved by the manufacturer datasheet. The fast diodes carrier lifetime plays an important role in changing V_F values. On the other hand, for a reverse direction operation blocking voltage is defined with (V_R) and accompanied by leakage current (I_R). Blocking voltage is a giving voltage by diode to block the current flow through it, the maximum blocking voltage the diode can handle without breaking down is called the maximum reverse voltage (V_{RRM}) followed by the maximum leakage current (I_{RM}). The physical breakdown of diode is known as (V_{BD}) due to a blocking voltage exceeds V_{RRM}, Figure (7) shows I-V characteristic of a fast 300-V pin-diode and its parameters defined in both forward and reverse processing measured at standard conditions of 25 ºC [19].

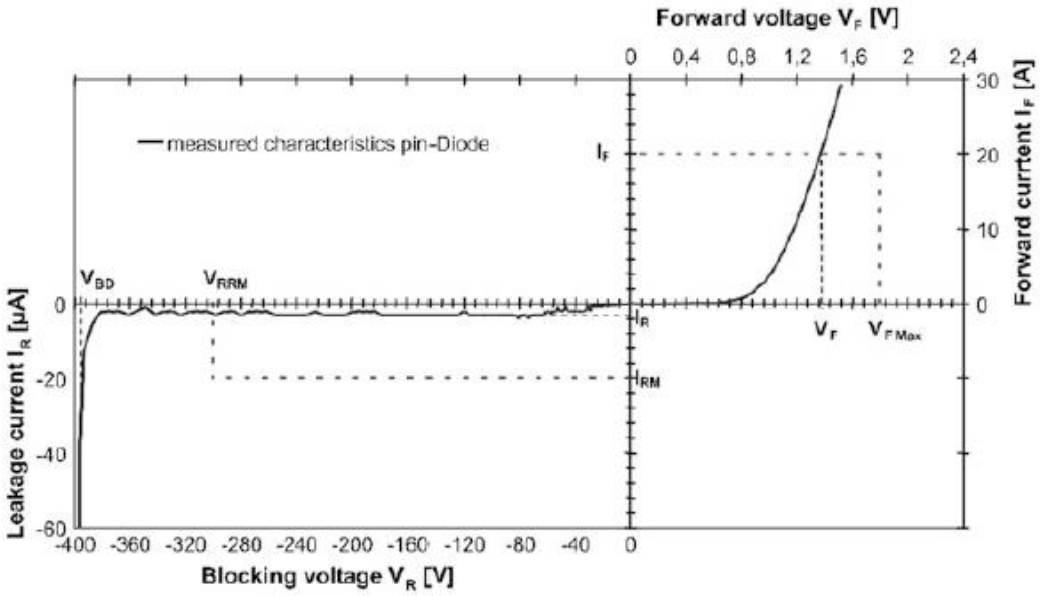

Figure (7) I-V characteristic of a 300-V fast pin-diode performance as well as some defined parameters [ibid.].

5.2 Thyristors

Among all other types of power electronic components, thyristors are distinguished by operating on high power rang and capability of blocking very high voltages and currents. The first thyristor was early introduced in 1956 followed by the constructing of a Silicon-Controlled Rectifier (SCR) which is still in use nowadays. Thyristors have wide range of applications, such as in low switching frequencies as controlled input rectifiers, yet the main application is on HVDC transmission systems [19]. In addition, the power thyristor has the ability to block voltage on both forward and reverse operation and provide stable characteristics, it allows low voltage drop during the on-state and low reverse current while blocking voltage in the off-state. For the time being power thyristors are such attractive devices for bulk power processing and play an important in HVDC systems, a single power thyristor device can block voltage of over 8KV and conduct current flow reaches to 5KA, which allows the thyristor device to apply control on 40 megawatts power. The thyristor consists of four doped layers constructed as P^+-N-P-N^+, where N^+-doped layer works as cathode layer and P^+ layer as anode. This can be represented as two coupled bipolar pnp and npn transistors which adds robustness to the device, and the four layers are formed through three junctions J_1, J_2 and J_3 as seen in Figure (8). The thyristor is structured using a slightly doped N-type silicon wafer whose thickness and resistivity vary depending on blocking voltage rating, then the four layers are formed by the diffusion of dopants form the frontside and backside of the wafer. The electrodes are placed on the frontside of the wafer to link the cathode layer with P-base regions, whereas on the backside to contact the anode region and N-base region stays with no attached electrodes [5]. During forward bias after triggering thyristor gate using a secondary voltage source between gate and cathode terminals, junctions J_1 and J_3 are heading to forward direction and J_2 is in reverse direction that allows conducting through the thyristor from anode to cathode as long as the device in the on-state. As a result of this, J_2 is affected by space-charge leads to a high electric field through the N-layer, hence thyristor works as a PN junction diode in forward bias. Switching off a thyristor is by applying a reverse voltage across it, when the reverse voltage is applied the junctions J_1 and J_3 are switched into reverse biased and junction J_2 is in forward biased that stops conducting and turns off the thyristor blocking any voltage on its terminals [19].

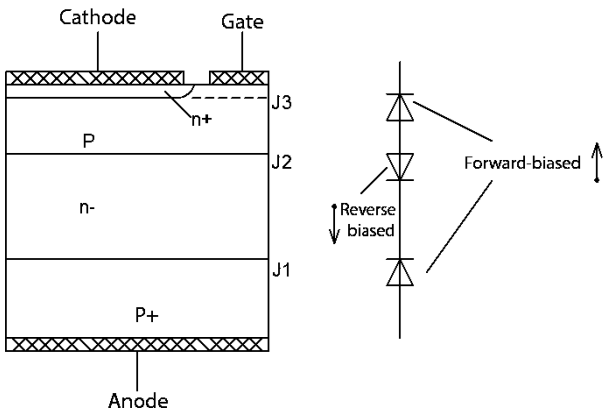

Figure (8) power thyristor structure and its operation modes [ibid.].

5.3 Silicon-controlled rectifier

The Silicon-Controlled Rectifier (SCR) is one type of thyristor-based power electronic devices, its basic structure consists of three terminals which are anode, cathode and gate. It can be turned on for forward bias operation by applying a positive current pulse (I_G) on gate terminal for a short duration, which is characterized by delay time (t_d), rise time (t_r) and turn-on time (t_{gt}) [44]. Delay time t_d is the transient time in which the anode current (I_T) rises to 10% of its final value where its voltage drops to 90% of its initial value (V_T). Rise time is the interval followed after delay time in which anode current rises from 10% to 90% of its final value and anode voltage drops from 90% to 10% of its initial value. Turn-on time is the time SCR takes to go from the forward blocking mode to forward conducting mode and it is the sum of all intervals including delay time, rise time and finally the spread time in which anode current keeps increasing from 90% to its final value and anode voltage decrease to its smallest possible value [11]. After the SCR is triggered in forward bias, it stays latched on until a negative anode current is applied to turn it off, which is generated by the utility voltage. During the turn-off process, the anode current starts to drop and is characterized by peak reverse recovery current, reverse recovery charge and two time regions which are the turn-off time and reverse recovery time (t_{rr}) [44]. The turn-off time is the total time taken by the anode current to fall to zero and the device is back again to its forward blocking mode. The reverse recovery time is the interval in which the anode current keeps increasing in reverse direction after reaching zero value, this helps to remove the stored carrier charges from junctions J_1 and J_3. Within a very short time the carries charge density decreases and cannot preserve the anode negative current any longer, hence it starts rapidly to rise in positive direction to reach zero again, the maximum value of the anode

negative current in reverse direction is called the peak reverse recovery current [11]. The SCR device can be used in various applications such as phase-controlled rectifiers for processing Pulse Width Modulation (PWM) current source inverters or load-commutated inverters that are used in synchronous motor drivers [44].

5.4 Gate Turn-Off (GTO) thyristor

Back to the 1980s, The Gate Turn-Off (GTO) thyristor was invented to overcome the limitation of using semiconductor devices for higher power and replace its competitor, the bipolar power transistor at that time for voltage ratings over 1400 V. Later on, the GTO thyristor was replaced as well by the Insulated Gate Bipolar Transistor (IGBT) for the same available power ratings, due to the high effort and requirements of turn-off process of the GTO thyristor and its drive unit. Yet the GTO thyristor is still being used nowadays for power ranges that cannot be reached by using the IGBT [19]. The GTO thyristor is a developed thyristor structure that can be controlled in a circuit of DC power source through a gate signal to turn it off or on, the turn-on process is the same way as in SCR device by applying a positive pulse of gate current, however for its turn-off process it is achieved by producing a large reverse gate current sufficient enough to sweep out the stored carrier charges in P-base region [5], hence the GTO thyristor is a self-extinguishable device. The GTO thyristor can be manufactured in symmetrical or asymmetrical structures and it is usually designed in press-pack modulation that provides higher cooling process. For symmetrical structure, it is distinguished by having a maximum repetitive peak off-state voltage (V_{DRM}) mostly equal to the maximum repetitive peak reverse voltage (V_{RRM}) and its capability of reverse voltage blocking as well, therefore it is using in current source converters, " V_{DRM} is the maximum value of an instantaneous repetitive off-state voltage that is allowed across the thyristor, where V_{RRM} is the maximum value of an instantaneous repetitive reverse voltage that is allowed across the thyristor without cause breakdown. On the other hand, an asymmetric GTO thyristor is more used in voltage source converters because the need of reverse voltage blocking is not required and it has a V_{RRM} value much lower than V_{DRM} [44]. The basic structure of the GTO thyristor is similar to that one of a typical thyristor, however the cathode layer has smaller width than it is in a conventional thyristor to ease the turn off process of anode current and the GTO does not contain any cathode shorts. Figure (9) shows the structures of a symmetric and an asymmetric GTO thyristor and the electric field shape resulted from blocking gate turn-off processing of each. The asymmetric GTO thyristor is fabricated by adding an N-buffer layer with higher doping concentration to the neighbor N- base region of the anode P^+ region, this results in forming an electric field profile different to that one of a

symmetrical structure, reducing the gain current through the pnp transistor and the turn-off time. The on-state voltage drop can be reduced by adjusting the thickness of N-base region and make it smaller in case of asymmetrical structure than in symmetrical one. Turning GTO thyristor off is accomplished by either a step function of gate current allowing a constant reverse gate current or through a ramp drive where the reverse gate current rises over time. For both types, the GTO thyristor takes a transient turn-off time called a storage time (t_s) at first within its regenerative mode, which can be reduced by increasing the rate of reverse gate current. After this storage time period, the anode voltage starts to rise significantly followed by a sudden decrease of the anode current represented as a long slow decay that is known as the current tail. The existence of high anode voltage over the current tail time duration causes large switching losses which is considered one of the GTO thyristor drawbacks and limits the frequency operation of the device [5].

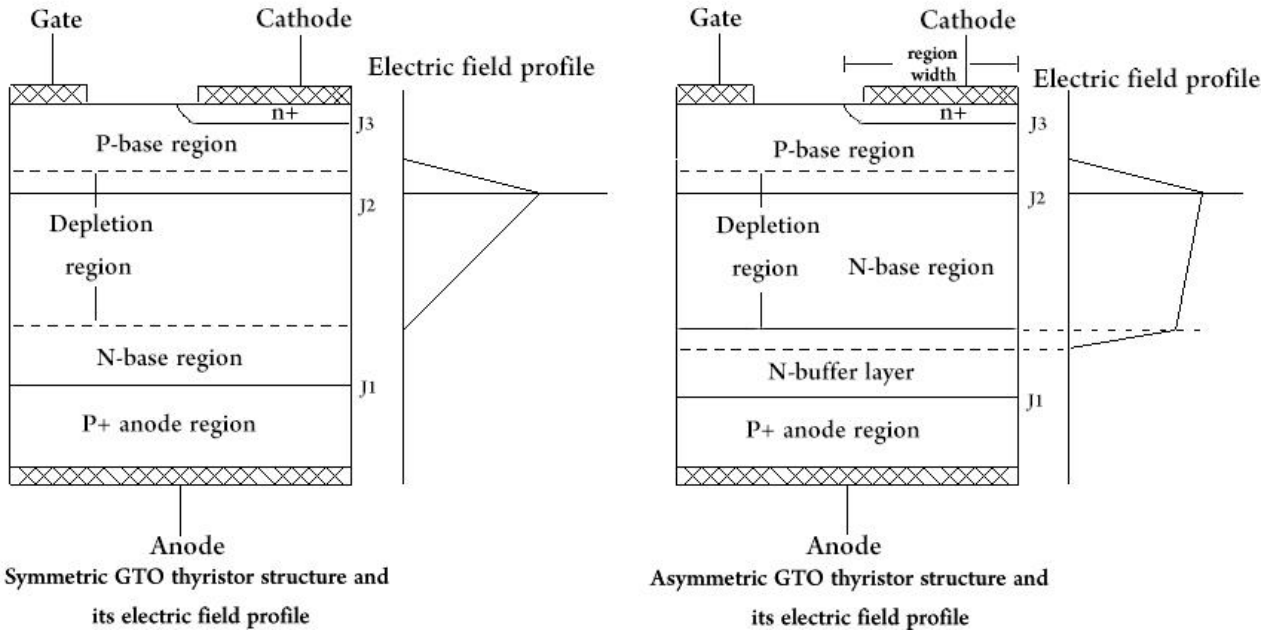

Figure (9) symmetric and asymmetric GTO thyristor structures in addition to their blocking gate turn off electric field profiles [ibid.].

5.5 Insulated Gate Bipolar Transistor (IGBT)

Insulated Gate Bipolar Transistor (IGBT) was the result of previous works that were done in 1980 on developing and combining operation processing of bipolar transistors and MOSFET, which became after a commonly used device for high power switching applications [5]. The

main aim of these works was to add the possibility of voltage control feature that is shown in MOSFETs to bipolar devices. However, its basic structure is also consisted of four layers, they are plunged in such a way that there is no regenerative thyristor is formed during its performance. Over time, after the IGBT was invented, it made a significant contribution to the market, replacing its previous bipolar power transistors and more recently with GTO devices for higher power ratings [19]. IGBTs are commercially available in two designs modular and press-pack, modular design is used mostly for high-power applications which is formed by an insulated baseplate with one-sided cooling whereas press-pack design which is differentiated with better cooling has limited selections for cost reduction. The IGBT is a voltage-controlled device that does not require gate current to turn on or off during its switching process, but the presence of capacitance between the gate and emitter requires a few amps of gate current to overcome switching transients. Switching IGBT on is done by applying a positive gate pulse voltage of +15 V, while switching it off when the gate voltage reaches zero. The voltage across the gate and emitter V_{GE} is equal to the gate voltage V_G but only occurs when the device is completely switched on or off, due to the gate-emitter capacitance V_{GE} is below V_G during switching transients , therefore a gate resistor is connected in series with the gate terminal as shown in Figure (10) to smooth the switching process [44]. In accordance with the power bipolar transistor structure, the collector is considered as the anode and the emitter as the cathode. As long as there is a positive voltage between the collector and the emitter, the device is in blocking mode. Once a gate voltage is applied, an n-channel is created and electrons begin to flow to the collector injecting holes of the p-type collector layer, causing a higher density of the charged carrier in the middle layer, which increases conductivity. Turning on or off an IGBT device mainly depends on that n-channel by creating it for forward bias connection or removing it for blocking mode operation. The development of IGBT has helped to spread its applications for different and higher rated voltages, enough to replace its previous devices in some applications like thyristors. Nowadays, IGBT devices with a high blocking voltage range from 3.3 kV to 6.5 kV are commercially available, making IGBT devices very well suited for use in HVDC applications. There have been several other developments to provide IGBT devices for a higher blocking voltage of 10 kV. However, these devices have not yet been released on the market. IGBT devices suffer from switching and conductivity losses, which can be reduced by lowering the forward voltage drop of the device. Some development works exemplify that IGBTs are likely to be available with a rated voltage range of 1200 V at a forward voltage drop of less than 1.5 V, thereby reducing device losses. Furthermore, IGBTs above 3 kV perform better than unipolar Silicon-Carbide (SiC) devices in terms of forward voltage drop. Although bipolar SiC

devices might be used, but they still exhibit some problems concerning incomplete ionization in the doped p-emitter layers. Further works and researches are underway to develop IGBTs to improve the ability to control higher power with less losses and also to make progress for SiC IGBTs [19].

6 Topologies of HVDC systems and applications

The high voltage direct current (HVDC) transmission systems are, in some cases, more suitable and economical to be replaced by the AC transmission lines in which they are superior to the AC system as previously described. As a result, HVDC systems have made great progress in HVDC applications around the world in recent years due to their advantages and properties. Several projects have been carried out using interconnections based on HVDC system technologies, either via voltage source converter technology or current source converter technology, each with its own characteristics (see Table (3) for comparison) through different topologies. These topologies offer new features, new converter techniques, better configurations and improvements for each technology to serve different purposes and to achieve the best results and the best performance.

6.1 HVDC transmission system topologies

Different topologies show various methods of setting up a HVDC link between two points, where the medium is represented as a single pole or bipole connected to the station converters that can be two-level or three-level converter configurations or a connection of multi-terminal. Apart from the converter technology itself, the medium link is constructed in two commonly used types monopolar HVDC topologies and bipolar HVDC topologies.

6.1.1 Monopolar and Bipolar topologies

In monopolar HVDC topologies, in which the name describes itself, only one conductor and mostly in negative polarity is used to reduce the effects of corona phenomena and the installation cost is reduced, while the costs for bipolar HVDC topologies are higher, since at least two converters are used at every station terminal, but can deliver twice as much power as monopolar systems. In order to reduce the harmonics on the AC side in bipolar systems, the converters are connected to the AC network via two transformers, whose secondary windings are configured once in a grounded star-delta arrangements and the other in a grounded star-

star configurations. Taking into account that the secondary windings of the transformers must be well insulated to withstand the high voltage stress from the grounded DC side. In addition, bipolar systems have the advantage of poles capability of being overloaded with more than half of the full transmitted capacity when fault occurs on one converter [16]. In general, there is one type of HVDC topology that has dominated most of its modern application, namely a bipolar system configuration where each pole is connected to a 12-pulse converter at each terminal. This balanced operation without flowing earth current enables two separated DC circuits, each of which can transfer half of the total capacity. For applications where the DC line voltage for bulk power transmission exceeds 500 kV, a series-connected converter configuration is used, as shown in Figure (10), to overcome the possibility of partial line insulation breakdown or converter outage failure [4].

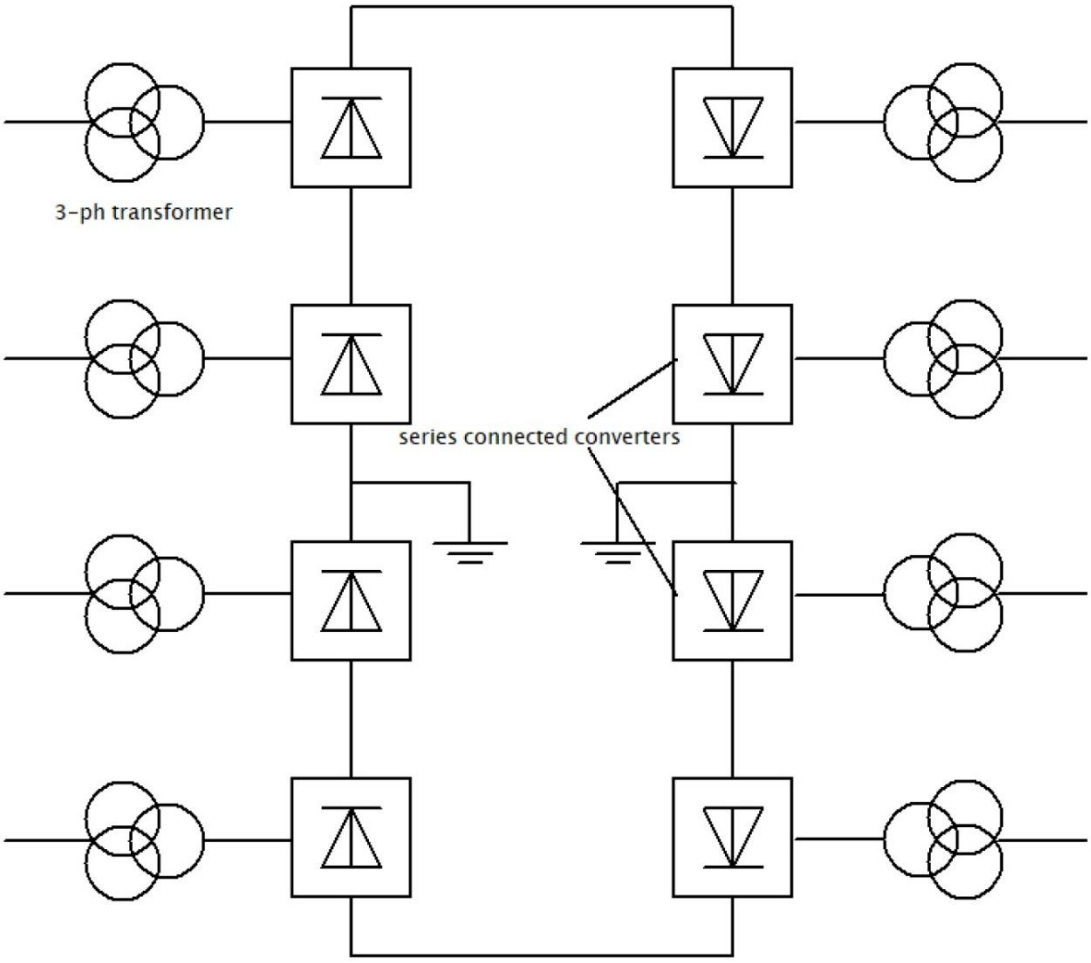

Figure (10) HVDC configurations of a bipolar series connected converters system [ibid.].

Previously two different topologies have been shown up in Figures (6-a, 6-b) which are an asymmetric monopolar with ground return and bipolar DC link with ground return respectively. There are three commonly used configurations for monopolar HVDC topologies:

A) Symmetric monopolar: Figure (11) shows the structure of this topology, in which the capacitors connected to the DC link in parallel are grounded at their midpoints, the two conductors used are completely insulated, which increases the installation costs and no grounding is used on the DC side. However, due to its symmetry design and operation, it offers some advantages since the AC transformer does not have to be complicated to construct because it is not exposed to the high voltage DC stress. This topology is the only topology that prevents AC side fault currents from flowing into the DC side when a pole to ground fault occurs.

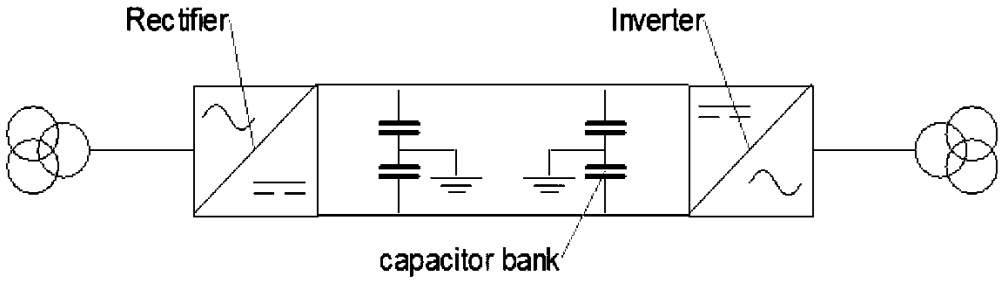

Figure (11) HVDC topology of a symmetric monopolar transmission system [16].

B) Asymmetric monopolar with ground return: As represented previously in Figure (6-a) it relies on grounding the DC side circuit, although this topology has the disadvantage of having a continuous earth current and requiring permission to install the electrodes, which can cause some environmental concerns, it still has two main advantages: the first is that only one conductor is used and the ground as return, which reduces installation costs, and the second is that it can be expanded to a bipolar connection if necessary [16].

C) Asymmetric monopolar with metallic return: This topology uses a metallic conductor as a return path, so no grounding is required, and this reduces the cost of using an insulated return conductor. It has an advantage in case of faults occur as partial collapse of the line insulation, because the metallic return has a small voltage drop that the remaining

good insulation parts can withstand. In addition, due to its structure as demonstrated in Figure (12), it can easily be upgraded to a bipolar system if required [4, 16].

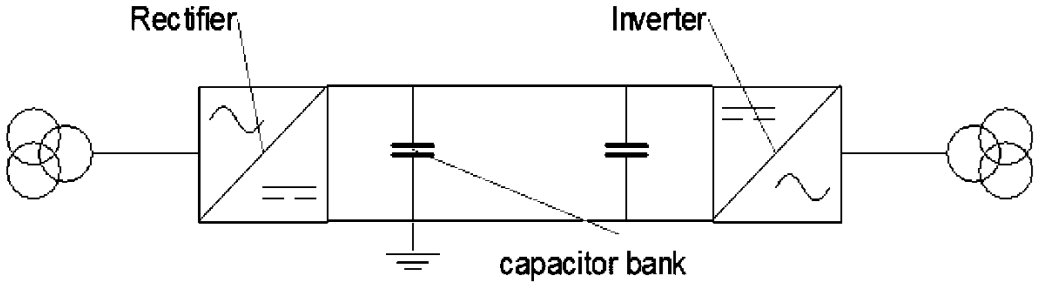

Figure (12) HVDC topology of an asymmetric monopolar transmission system with metallic return [16].

On the other hand, bipolar HVDC topologies are mainly divided into two different configurations:

A) HVDC bipolar system with ground return: Previously in Figure (6-b), which shows a block diagram for this topology, with some additional cost than monopolar systems, another insulated conductor and more converters are used. Obviously, the DC circuit must be grounded, which raises some environmental concerns due to ground currents, either to protect against faults or in unbalanced operation, or under normal conditions as part of bipolar system configurations. If a fault occurs and no return path is provided, the system must be temporarily shut down until the fault is cleared.
B) HVDC bipolar system with metallic return: This topology is similar to its counterpart, the bipolar system with ground return, but the difference is that a low-resistance insulated metallic conductor is added. It is used in cases where ground return is not possible and helps with faults such as pole outages or carrying out some maintenance by using the metal wire as a return, although there are additional installation costs [16].

6.1.2 Multiterminal HVDC topology

In addition to the previous topologies, a further trend of HVDC system topologies has been implemented, which has been able to pay close attention to HVDC applications, especially for the integration of offshore wind farms in AC networks with good stability, robustness and cost reduction. This trend is known as multi-terminal HVDC topology (MT-HVDC). Since VSC-based HVDC is characterized by the ability to withstand voltage drops on the AC side and thus avoid

commutation failure, besides that the power direction not only changes by reversing the current direction, but also the voltage polarity does not have to be reversed, as in the case of a CSC HVDC System. Therefore VSC-HVDC systems are often chosen and more practical in MT-HVDC applications.

It is taken into account that many factors evaluate different topologies of MT-HVDC networks and give a complete assessment for each topology before the installation process begins, e.g. the capacity of DC circuits, cable length, transmitted power capacity, the ratings of VSC stations, stability requirements, types and operating ratings of circuit breakers, network flexibility, robustness of the system, availability of the source and installation costs. Moreover, three standard principles are selected for the integration of offshore wind farms in onshore AC networks, in which the MT-HVDC topology is the best economical option for remote implementation, to ensure a successful performance of such a system. These conditions are introduced by Great Britain's security and quality of supply standard (GBSQSS) which are presented below:

1) Flexibility in regulating the DC voltage under both in normal operation and in the event of a fault.
2) System reliability in case of faults, if a fault occurs, the MT-HVDC grid should continue to support the AC grid and should not cause a complete power failure.
3) If a converter station outage occurs, the MT-HVDC control system must be able to supply at least a certain value, referred to as the maximum power failure (1320 MW according to Great Britain), under these circumstances [30].

A variety of MT-HVDC topologies can be used in offshore wind farm applications based on an HVDC transmission system. Some of these are used in AC networks and the selection depends on the operating conditions and the type of DC faults or converter station outage that are likely to occur in each topology. Some of the most important topologies used are explained below:

6.1.2.1 Point to point topology (PPT)

This topology is represented as multiple DC links with each offshore wind farm in point-to-point connections with the onshore grid side. However, it has a different configuration than the other multiterminal topologies, it still belongs to them as it allows continuity of the power flow in the event of a fault. In case of converter outage or DC circuit failure, the followed procedure is to open the circuit breaker associated with the faulted line to disconnect it and set the turbines to trip off. If there is a line fault in a wind farm connection, it will cause blackout of this wind farm.

Therefore, this type of topology lacks a main principle regarding flexibility [13]. Nevertheless, there are currently more than 200 point-to-point carried out projects worldwide [30].

6.1.2.2 Wind farm ring topology (WFRT)

WFRT is seen as a revolution in PPT by adding more flexibility and control to the power flow. This is done by placing wind farms in a ring, the number of DC circuit breakers of which corresponds to the number of wind farms, which reduces the number of circuit breakers required [13]. The DC circuit breaker opens as soon as a circuit fault occurs disconnecting the substation and the associated VSC side linked to the faulty wind farm. Then an isolator operates to detach the entire faulty region with fault current, the DC circuit breaker recloses again once the fault current is cleared and the system is back again to normal operation. Yet, in case of presence of fault on the grid side of VSC, it leads to an increase in the DC link voltage and thus impairs the flexibility and reliability of the system. Furthermore, if the fault occurs on the wind farm ring itself, the DC circuit breakers of the faulty region open to disconnect it, as a result of that an offshore wind farm and an onshore VSC are out of service. This increases the maximum power failure to a value that might not comply to GBSQSS criterions [30]. Although the procedures in the event of a line fault are similar to PPT and cause temporary insulation of the faulty line connected to the associated wind farm, this wind farm can be reconnected to another substation thanks to the ring construction. In general, WFRT is more flexible and robust than PPT because it can handle faults on any line without cutting power off completely. However, this requires fast commutation and a coordinated sequence of HVDC protection devices [13].

6.1.2.3 Substation ring topology (SSRT)

SSRT is a ring topology and therefore has a configuration similar to that of WFRT. The main difference, however, is that the ring at SSRT is installed on the onshore side on the grid side of VSCs. Each wind farm with its converter is connected to a power converter station on the mainland, and all these stations are connected in a ring by protective devices as isolating switches and circuit breakers. During a DC fault, the procedures result in one of the mainland stations being disconnected with respect to the fault and the corresponding wind farm, which increases the maximum power loss indicated by GBSQSS [30]. This configuration provides more flexibility on the AC mainland grid than on the wind farm side in the event of a fault or for maintenance purposes. The wind farm's HVDC-VSC is isolated if a HVDC line fault occurs, resulting in a loss of flexibility on the wind farm side and deprive the wind farm of its full performance. This makes the WFRT superior to the SSRT in most applications because WFRT

offers greater flexibility that ensures the continuous operation of wind farms despite the presence of faults in the HVDC circuits [13].

Furthermore, other MT-HVDC grid topologies and some proposed ones with simulation results are illustrated by Refs. Some comments on the comparison of the previous different topologies initially refer to the number of circuit breakers required. This shows that circuit breakers are not required for PPT, while for WFRT and SSRT the number of circuit breakers corresponds to the number of wind farms or mainland stations. Second, the circuits rated power of each topology which economically affects the choice of topology. The circuits are designed for the same power of the included converter to which they are connected. This applies to PPT and some other topologies known as star topology (ST) and star with a central switching ring topology (SGRT), which is a hybrid configuration takes the advantages of both ST and general ring topology (GRT). In the case of WFRT and SSRT, the circuits are designed for the same rated power of a single station between the offshore and onshore side and rated twice for the ring circuits. eventually, there is the flexibility of the topology and which parts of the system are disconnected in the event of a long-term fault. Within a PPT fault, a single wind farm is completely out of service. If faults occur on one of the WFRT offshore to onshore lines, a substation is disconnected whereas a wind farm for SSRT is disconnected [13].

6.2 Applications of HVDC transmission system.

The HVDC transmission system has several advantages that make it suitable for applications that are normally related to renewable energy sources, since in most cases they are remotely sited and require transmission power over long lines. This also helps to increase the chance of using more global resources with a small power-area ratio. The HVDC system has the ability to overcome some setbacks that its rival, the HVAC, faces. For example, HVDC can have a higher output per conductor and does not suffer from problems due to frequency fluctuations, resonance and above all the robustness of the system, which do not depend on the distance between the source and the demand center [16]. In general, the installation of a HVDC system helps to reduce the cost of the transmission system per MWh for distant projects beyond the specified breakeven distance and to dispense of the use of intermediate switching stations or reactive power compensation units, as is the case with HVAC systems. In addition to increasing the flexibility of the system through more precise controllability of the power flow and for parallel transmission by eliminating the loop flow, which increases the capacity to supply local generation points and intermediate loads [4].

6.2.1 Asynchronous DC ties

Interconnections between two networks with either the same frequency or at difference frequency can be carried out by attaching an asynchronous DC link to tie these networks. It is done for grids where they tend to be weak and do not show the full transmitted power. Among the two HVDC technologies, the HVDC-based VSC is more preferable due to its ability of fast recovery from faults that might occur on the AC linked grids, avoiding commutation failure and smooth operation of reversing power flow direction if required for efficient economic power flow [3]. The DC tie protects the system from any outage failure that might occurs on one network preventing it from propagating from the faulty network to another. For instance, back in August 2003 in northeast America, where a blackout occurred on the AC interconnection between New York and New England, an ascending outage expanded through Ontario and New York and kept propagating until Quebec where it interfaced with the DC link and stopped there, Quebec stayed unaffected and continued to deliver power via the HVDC links to New England. This asynchronous connection refines the connection between the two networks with mutual benefit and in many cases takes place via back-to-back converters. Some examples of asynchronous interconnections already installed in North America are between the eastern and western systems, between New England and the Maritimes, and interconnections between the Mexico network and the Southwest Power Pool (SPP) network [4].

6.2.2 Long distance and submarine cable transmission for bulk power

A typical HVAC transmission system requires more power lines and higher costs than an HVAC system relative to long distances, e.g. for some distant hydropower plants or wind farms that transmit bulk power. HVDC is superior because it can use fewer overhead lines to deliver the same power as an HVAC system at a lower cost with no issues and less losses, therefore HVDC is more economical for long distance. The bipolar HVDC transmission system can supply electricity as a double-circuit HVAC system, since each DC line can carry up to half of the total transmitted power. The level of the DC transmission line voltage plays an important role in losses along the DC line. The higher the DC voltage level, the lower the losses on the transmission line. Thanks to higher level of controllability of the UHVDC system, it is therefore selected and is favorable for applications for bulk power transmission over very long distances [4]. UHVDC has a voltage level of ± 600 to ± 800 kV. Submarine cables are the alternative form of power supply when the land cables are expensive due to transport and RoW restrictions. For underground or submarine distances over 40 km, which tend to cause high installation costs

due to long distances, extruded HVDC cables are best suited for such applications. They are characterized by flexibility, lower costs, lightness and simple splicing over long distances that helps to reduce installation costs and make it feasible for long underground transmission cables [3]. Furthermore, an underground AC line suffers from charging current over a distance due to the high capacitance and lower inductance of its reactive components. Although this can be overcome by adding additional costs by placing a set of shunt capacitors, this method is only suitable for underground cables and not practical for submarine cables [ibid.].

6.2.3 Multi-terminal connections and large scale infeed

With the help of HVDC transmission line technology, systems with multiple connections are easier to design, control and become more reliable. In general, in conventional multi-terminal systems, power reversal is accomplished by reversing the voltage polarity, which might require additional costs and steps to reverse the polarity, such as switching a converter to reverse the voltage polarity. Yet, VSC-based HVDC is best for multi-terminal connections because it simplifies the process by reversing only the current direction on a line connected to the intermediate tap, which results in power reversal and no polarity reversal is required regardless of the main power [3]. The power supply of large cities and as well as the inflation of urban cities, which increases the demand for loads, mostly relies only on the old and inadequate power plants in the vicinity of the cities. Not to mention the emissions from these less efficient plants compared to the newer units, which are relatively far away. Providing adequate performance with high reliability can be done via VSC-based HVDC underground cables, since RoW is limited in urban cities and land use can be avoided. This works in order to deliver more power, regulate the voltage for the robustness network and provide a reactive power reserve, since the receiving ends work as virtual generators. The VSC station is compact and can therefore be housed and placed indoors for an aesthetic view in cities. The VSC-based underground circuits can be installed in an existing RoW to ensure an economical dual use for better performance [4].

6.2.4 Offshore and insular load power supply

Offshore loads are sited remotely from any utility, so gas or oil power units are used to supply power to feed them. These units incur high operating as well as they are less efficient and cause air pollution due to their emissions since they depend on the operation of oil or natural gas. VSC-based converters are compact and can be used as a replacement for these oil units. The converters can work efficiently with variable frequency to meet all load inputs such as high

voltage motors and large pumps. Further, isolated local loads can be powered over long distances on remote islands using VSC-based HVDC submarine cables. The VSC-HVDC transmission system supports black start, better control and voltage regulation and works without commutation errors. The same scenario applies to large offshore wind farms. The associated transmission system must take environmental concerns into account over long distances. In addition, the power generation arrays of windfarms require reactive power support during the operation, which is why VSC-HVDC are best suited for such transmission systems. The VSC-based HVDC transmission system can support reactive power over long land distances or submarine cables and keep the difference in reactive power due to the conversion process within a certain gap so that the AC voltage of the adjacent network remains stable with the desired tolerance [3].

7 HVDC cables

Extruded cables are widely used in HVDC transmission systems and have evolved over time with the choice of cross-linked polyethylene (XLPE) as the best insulation material for these cables. However, these HVDC XLPE cables have two main problems that should be addressed, namely space charge accumulation and DC conductivity properties. During the manufacturing process and the introduction of insulation material, the crosslinked by-products can form cavities which lead to a change in the space charge behavior while in operation. A degassing process is therefore applied during manufacturing to keep the level of by-products content low [31]. In case of a high accumulation of space charge within the insulation material, this leads to weakness of the DC cables and their reliability. The gradient temperature across the cables is also increased through insulation layer due to the high current flowing through the cables. The XLPE material is characterized by several factors that make it the most suitable insulation material for high-voltage DC cables, such as, high dielectric strength, excellent physical and electrical resistance properties, since it withstands high moisture and cracking. Yet, it shows some limitations in the presence of space charge generated when a high electric field is applied to the insulation material. This results in ionization of the impurities within the material, changing the dielectric material load, which later leads to early degradation of the material itself and accelerates it to breakdown. These space charges injected at the electrodes mainly depend on the gradient temperature level and the electric field strength. The space charge density is measured using a modified pulse electroacoustic system (PEA) that shows space charge distributions through a cable sample connected to a HVDC supply and running through a current transformer as shown

in Figure (13). During the operation, the current transformer works on increasing the gradient temperature within the XLPE insulation material and thus heating up the cable via induction heating [43].

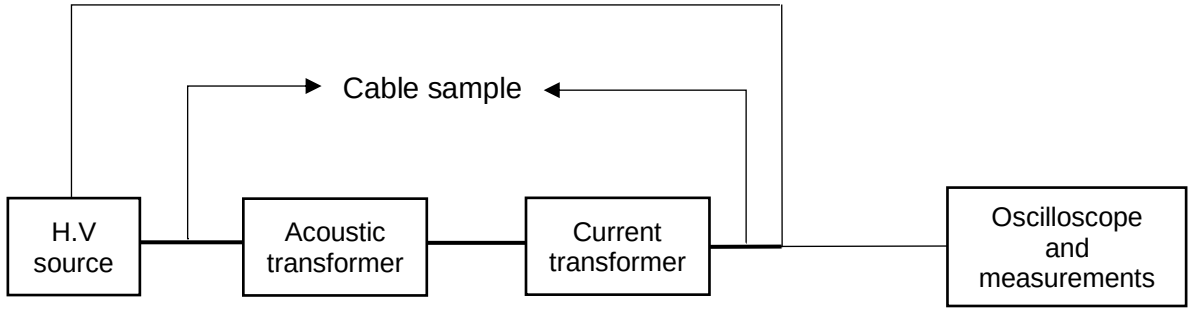

Figure (13) block diagram of PEA system for investigating space charge behavior of a cable sample [ibid.]

7.1 Space charge distributions

Several experiments were carried out on an HVDC-XLPE cable to investigate the behavior of space charge distributions. First, a cable sample was cut into 0.2 mm thick slices. The space charge density was measured by PEA system with applying electrical voltage ranges from 30 kV / mm to 50 kV / mm and over different time intervals at room temperature. These slices are distinguished by three insulation layers as shown in Figure (13) named inner, middle and outer layer respectively.

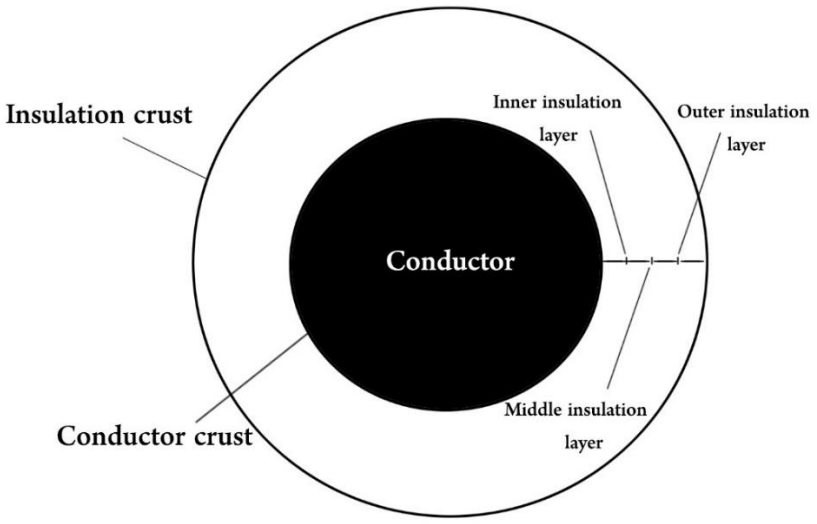

Figure (14) illustration scheme of insulation layers for an XLPE cable specimen [31].

In this experiment, results for non-degassed and degassed cable samples were taken. The degassing process was first carried out on cable cores at 70 ° C for 10 days. After a voltage is applied, hetero charges are formed near the cathode and anode in both degassed and non-degassed samples. With degassed samples, however, it can be clearly seen that they are low. In contrast to homo-charges, these hetero-charges have an opposite polarity to the neighboring electrode. Hetero-charges are said to result from the decomposition process of the remaining by-products in the insulating material into cumyl alcohol, acetophenone, water, α-methyl styrene and methane, all of which are sublimed during the degassing process, which is why the hetero-charges are reduced in degassed samples. The application of the degassing process over several time intervals of 0, 5, 10, 15, 20, 25, 30 days respectively has shown that it is effective to reduce the accumulation of space charges when it is applied for a certain time. This will help to improve the local distribution of the electric field, since the accumulation of space charges can easily distort it. It is noticed that hetero charges are mainly present in the inner insulation layer and are obviously reduced by increasing the degassing time from 5 to 10 days. However, for degassing periods longer than 15 days, and particularly for 25 and 30 days, the space charge density curve tends to have an increase peak. The mean space charge density curve is relatively low for the inner insulation, where it has usually a higher degree of distortion than the middle and outer layers, and that for degassed samples from 10 to 20 days. The distortion level is seen to be around 45.97% in inner insulation layer at 30 KV/mm for longer degassing of 25 days and it increases beyond 30 days up to 80%. The middle and outer insulation layers have less than 20% distortion level and their mean density curves are relatively steady for degassing of 10 to 20 days and at 30 KV/mm. In case of electric stress of 50 KV/mm, it is observed that the level of distortion in all samples, in particular in the inner insulation layer, has higher rates. The mean charge density curves are similar to that of a voltage stress of 30 kV/mm, except for longer degassing process exceeds 25 days [31].

In another experiment and with the help of the PEA system, the behavior of the space charge accumulation on DC cable samples was investigated by measuring the space charge density in two different temperature gradient test setups. The measurements were taken for several samples of a cable with a conductor 95 mm^2 and XLPE insulation material of 3.4 mm thickness. The samples have dimensions of r_1= 5.8 mm (inner radii), r_2= 9.2 mm (outer radii) and same insulation material thickness by applying voltage at 80 KV to the samples with respect to time after The test was set to a temperature gradient of 10°C using a 250 AC current transformer. Taking into account the fact that the cable samples were not subjected to a degassing process and therefore contained a sufficient amount of cross-linking residual by-products. When voltage

is applied between the anode (inner electrode) and the cathode (outer electrode), it is observed that a large amount of hetero-charges forms within the insulation layer adjacent to the anode after 1 hour. Later, after 3 hours, positive charges accumulate around the middle of the sample towards the cathode. A high rate of negative charge accumulation is found on the cable samples due to one of two reasons or a combination of both. The first reason is that negative charge can be trapped much easier than positive charge. The other reason could be that more negative charge is injected into the samples than positive charge. Since the positive charge around the sample is difficult to capture, it is attracted to the cathode vicinity rather than the anode vicinity. The accumulated positive charge near the cathode is eliminated or can recombine with the negative charge. The rate of accumulation of both negative and positive charges increases significantly by increasing the voltage duration up to 20 hours and then it settles down. With voltage-off measurements, slow movements of trapped negative and positive charges, negative charge next to the electrodes and positive charge around the middle of the sample are shown over the insulation material. Furthermore, the space charge decay profile shows a very slow rate after removing the voltage after 9 hours and short-circuiting both electrodes, while a small amount of negative charge on neighboring electrodes and positive charge in the middle is still present after 24 hours of decay [43].

7.2 Current distribution in DC power cables

When a DC flows through a conductor, it induces a magnetic field inside and outside that conductor. These magnetic field fluxes are perpendicular to the current direction and can cause a force on moving charge carriers in the conductor, which is called the Lorentz force. This leads to a Hall effect due to a radial electrical potential within the conductor. Considering a contour C around a conductor where a DC current I, the induced magnetic field β inside and outside this conductor is represented with the following Eq (1).

$$\oint_C \beta \cos(\alpha)\, dl = \mu_0 I \qquad (1)$$

Where μ_0 is the permeability of free space, dl is a radial length of the contour w.r.t the induced magnetic field and α is the angle between dl and β. To measure the potential difference between two points on the inner surface and the outer point in a hollow long conductor, an experiment was carried out by drilling a hole in the conductor as illustrated in Figure (15), the

axis of which is perpendicular to the axis of the cylindrical conductor. So that the magnetic fluxes induced by the hole point in the opposite direction, since the conductor is therefore divided into two parts in this area and the current flowing through them induces magnetic fluxes in opposite directions, which in turn partially cancel each other out. As a result, any net charge is also cancelled out and the potential difference can be measured between a point on the hole surface and a point on the boundary of the conductor.

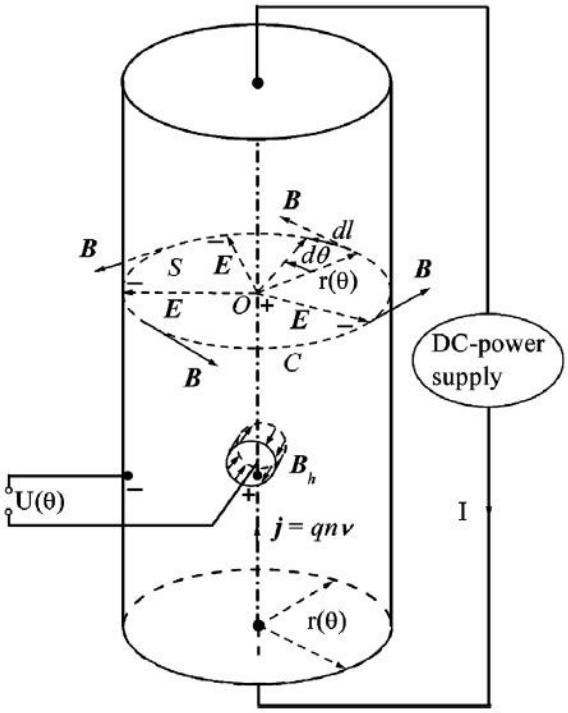

Figure (15) schematic representation of radial electromagnetic fields in a hollow long conductor carrying a steady current [49]

Moreover, Since the magnetic field β is perpendicular to the current direction and the charge carrier as well which moves in a path of velocity v, hence Lorentz force is affecting on the charge carrier path with amplitude of $q.v.\beta$, where q is the electron charge, resulting in building up a radial electric field in the conductor due to electron accumulation on the boundary by Lorentz force. The electric field E exerts a force qE on the charge carrier that opposite to Lorentz force, both forces are balanced under an equilibrium state and E is perpendicular to β. A radial electric potential difference U is present from the center of the contour and the end of the radial vector r, the mean potential difference $\overline{U}$ between any two points within area S enclosed by the contour and at any direction is obtained from Eq. (2)

$$\overline{U} = \frac{\mu_0 I^2}{2\pi q n S} \quad (2)$$

As seen from Eq. 2 that the mean potential difference between any two points within the enclosed radial range is proportional to the square of the current flowing through the conductor. The experiment shows that the potential difference along the current direction is proportional to the quadratic of current and is negligible between two points if their linking line is perpendicular to the current direction. The potential difference for a hollow long conductor is expressed by Eq. (3)

$$U = \frac{\mu_0 R_H I^2}{2\pi^2 (r_1^2 - r_2^2)} \quad (3)$$

Where r_1 and r_2 are the inner and outer radius for the conductor respectively. The measurements indicate that the potential at a point on the hole surface is always greater than that at a point located at the conductor boundary region. Furthermore, it is observed that the electrical potential is constant along a closed contour plane that is perpendicular to the current direction of a single conductor carrying a constant current, which indicates a homogeneous charge distribution in the conductor due to the absence of a skin effect in DC conductors [ibid.]. To ensure this, however, the current distribution must be uniform, which is seen as a problem with high-temperature superconducting (HTS) power DC cables. These cables are manufactured with multiple tapes to provide parallel paths for current through them. In order to achieve a homogenous current distribution, the current sharing among these various tapes must be uniform. This variation of the current distribution can be related to the critical current value in each band, which in turn varies over the cable length and can reach up to 10% in a band reel. The uneven current distribution due to these fluctuations leads to lower safety margins and critical damage to cables, which affects the aging process of the cable depending on the thermal capacity of the cable, since gas-cooled helium cables have higher potential damage due to their lower thermal capacity. A model of an HTS cable was used in an experiment to study the behavior of current sharing and the generated magnetic field in each tape. The experiment was firstly performed on the cable sample of twelve tapes and the results were analyzed using the Finite Element Method with the help of a commercial software, MagNet. The results show the distribution of the magnetic field on the cable tapes, which is shown in three

scenarios, as shown in Figure (16). The first scenario in Fig.16 (a) a uniform magnetic field in the cable sample as a result of a uniform current of 100 A in each tape. The second scenario, as shown in Fig.16 (b), non-uniform magnetic field profile due to an imbalance in current distribution in all the tapes in the case of an abnormal current of 0 A flowing through one tape and the rest of 100 A. The third scenario is represented in Fig.16 (c), a completely non-uniform current sharing in all tapes leads to a non-uniform magnetic field profile which influences the critical currents of each tape afterwards.

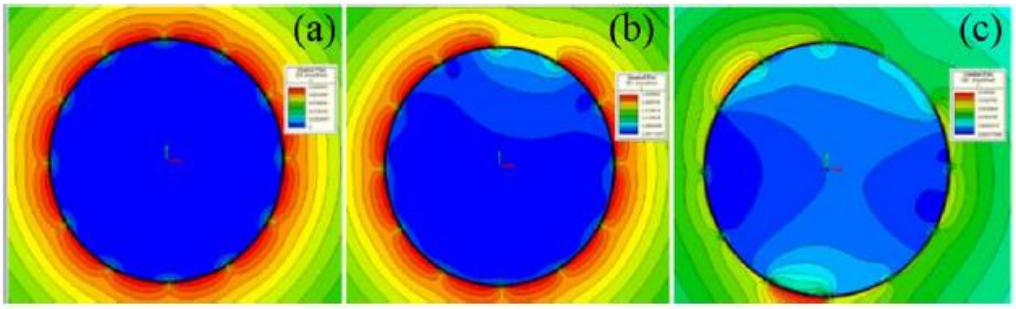

Figure (16) magnetic field distribution of an HTS DC power cable sample. (a) uniform current sharing. (b) non-uniform current sharing due to 0 A of a single tape. (3) non-uniform current sharing of all tapes [15].

Furthermore, a test was conducted on a sample of 4 tapes to study specifically the critical current distribution among the tapes by measuring currents and voltages in each tape while ramping the current from zero to 550 A. It is observed that for the first 22 seconds, a uniform current sharing between all tapes which is about 420 A. Tape 4 is seen to have the lowest critical current of about 95.9 A, since the current continues to increase, it cannot take anymore and transits to the normal state. However, the current flows through the remaining tapes, tape 4 does not share with any more current because it has already reached its critical current value. Tapes 2 and 3 show the same critical current of 108 A, hence having the same voltage profile and show the same behavior after they have reached their critical current without sharing further currents. Tape 1 has the final transition to the normal state and continues to carry the rest of the ramping current until its critical current value as tapes 2, 3 and 4 share constant currents up to their own critical current as shown in Figure (17). This performance of current distribution between all tapes is considered to be a high risk for large cables when tapes with a lower critical current constantly carry the current close to their critical values and below the total critical current value of the cable, which can lead to potential damage in the cable. Therefore, when

manufacturing HTS cables, the uniformity of the critical current distribution across all tapes must be considered.

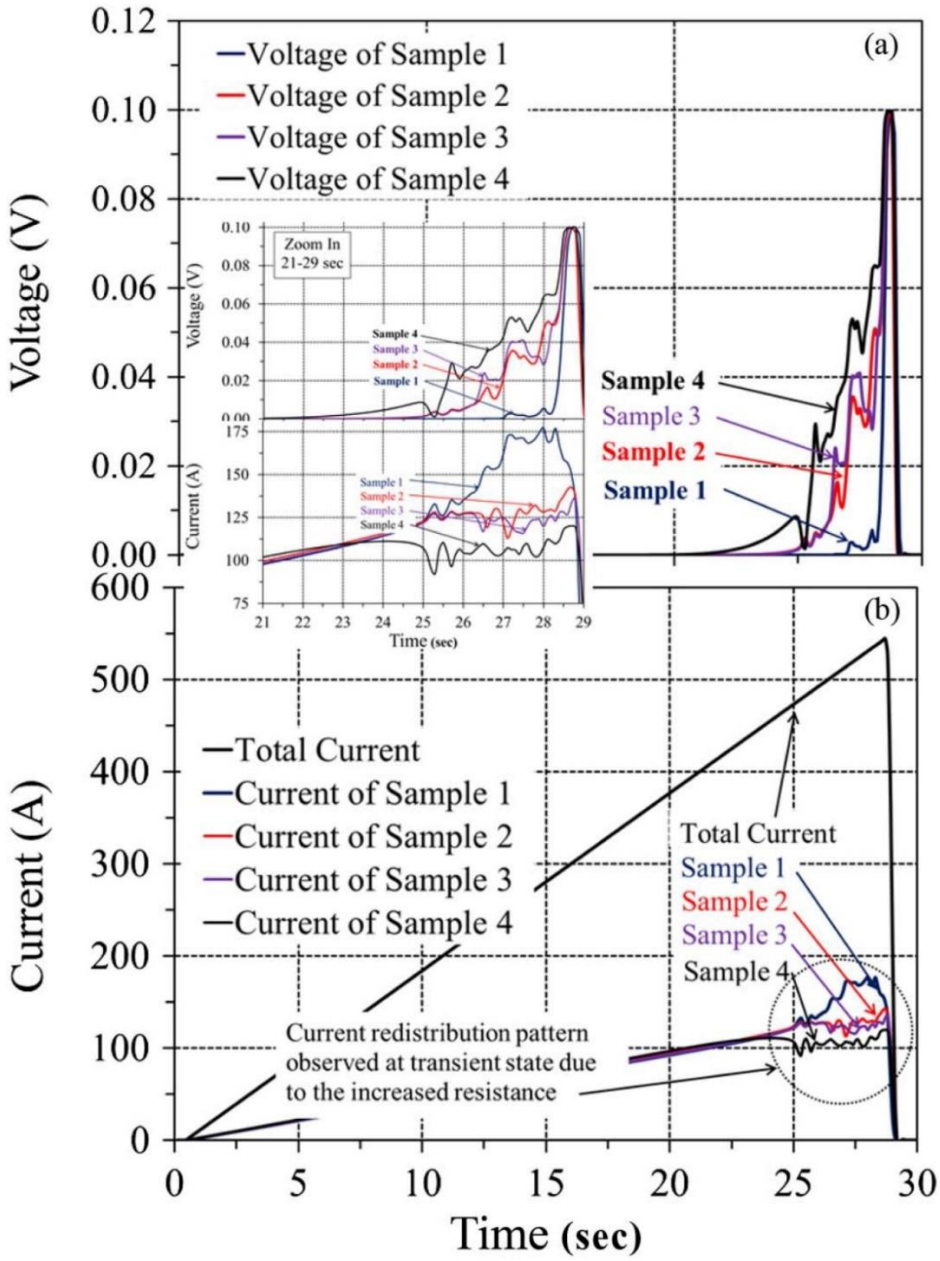

Figure (17) current-voltage characteristics of the four tapes of an HTS cable sample [15].

To study the magnetic field effects in submarine cables, a report by Collaborative Offshore Wind Research in the Environment (COWRIE) shows the results and measurements for a single unshielded DC insulated conductor immersed in seawater and for a bipolar DC cable with a

charged conductor positive voltage and the other as the return path. The report shows the relation as well between the magnetic field and the electric field which is derived from the measured magnetic field by the following formula:

$$E = 2\pi f B \quad (4)$$

Where:

E: the electric field (V/m)

f: power frequency (Hz)

B: magnetic field (tesla)

The report explains that for a single DC cable, the highest electric fields are in the cable insulation, where it has the lowest permittivity. Figure (18) shows a model for a single submarine unshielded DC cable in which, for simplicity, the relative permittivity is assumed to be constant. First, both capacitances for the insulation layer and the sea are determined in order to measure the potential at the interface point between cable insulation and sea, hence the electric fields in seawater and the cable insulation using equations for coaxial conductors. The maximum magnetic field around the cable is expressed by

$$B = \frac{I\mu_r\mu_0}{2\pi r} + B_{earth} \quad (5)$$

Where:

μ_r: relative permittivity of medium (assumed to be constant=1)

μ_0: Permeability of free space ($4\pi \times 10^{-7}$ N/A^2)

B_{earth}: earth's magnetic field (average value of 50 μT)

In the case of a perfectly metallic shield is applied around the insulation, only the electric field can be contained, but the magnetic field remains released in the sea because it is time invariant.

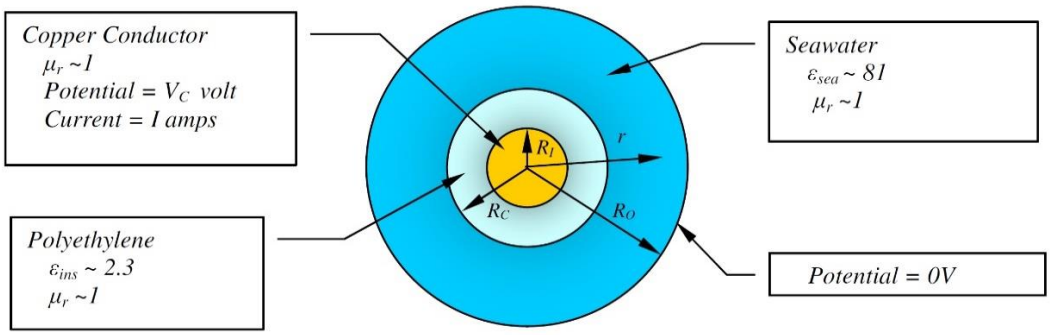

Figure (18) model of a single submarine unshielded DC cable [35].

A submarine bipolar DC cable has two conductors arranged side by side, one carrying positive current and the other negative current. Bipolar DC cable is believed to be the preferred practical method of transmitting energy across the sea as it can eliminate likely high electric fields in the sea associated with sea electrodes and help reduce electric and magnetic field levels. Consider a point P is located at distance R_1, R_2 from each conductor respectively, which shows the resulted magnetic and electric fields from each conductor. Figure (19) shows these vectors represent electric and magnetic fields components as a function of the radius R and the angle θ derived in X, Y domains, all components are resolved as functions of r and θ. The resulted equations show that the maximum levels of electric and magnetic fields in the sea can occur when $\theta = 0°, 180°$, whilst the minimum fields that head for cancellation occur when $\theta = 90°, 270°$.

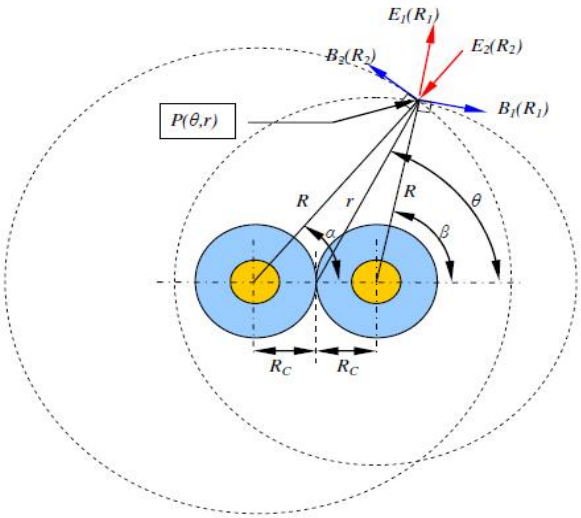

Figure (19) components of electric and magnetic fields [35].

Figure (20) demonstrates the maximum normalized electric and magnetic fields in relation to the distance from an unshielded bipolar DC cable axis compared to a single DC cable, which shows the degree of fields cancellation. Moreover, the cable is typically buried to a depth of 1 meter in the seabed, especially in shallow water, to provide more protection and increase cable lifespan. In this case, the magnetic field surrounding the cable remains untouchable, since it is only surrounded by the seabed and sea water, both of which are not ferromagnetic and therefore have an approximately unity magnetic permeability. The electric field around the cable will be depending on the conductivity and permittivity of the medium.

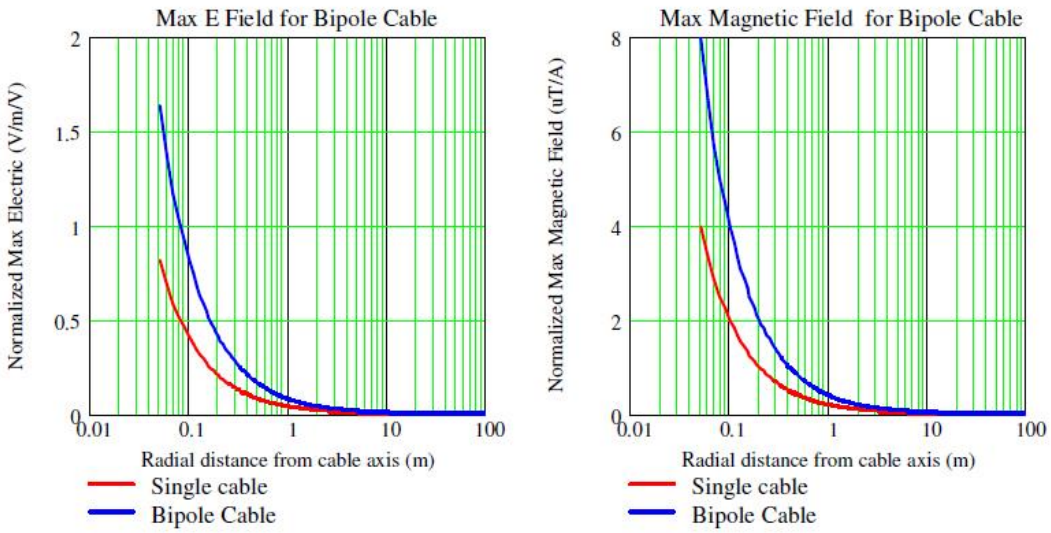

Figure (20) electric and magnetic fields with respect to distance from unshielded bipolar and single DC cable axis [35].

7.3 Electromagnetic interference in parallel transmission lines

The main theory of electromagnetic coupling between HVDC and HVAC lines results from the mutual capacitance and inductance between the power lines, which leads to the generation of coupling voltage and current on the HVDC lines [18]. Due to the constantly growing power demand, HVDC transmission lines with the ability to transmit mass energy with high reliability are required and have made a large contribution in power transmission systems. However, the RoW (right of way) is not always sufficiently available for a completely new transmission system, and therefore HVDC lines share the same RoW in many applications with AC systems that have already been built. This leads to an interaction of the electromagnetic field to the close distance from the inductive and capacitive coupling of parallel AC lines on the neighboring DC lines,

which leads to induced voltage upon the HVDC lines that might cause insulation failure of the converting connected equipment to the HVDC system. In a model that represents a hybrid system based in China of a three-phase AC transmission system (500 KV over 200 Km) alongside two conductors that represent positive and negative lines of a DC system (±800 KV over 1446 Km) as shown in Figure (21), the electromagnetic interaction is calculated for a spatial proximity varies from 50 to 240 meters for analysis purpose using an electromagnetic transition program (EMTP).

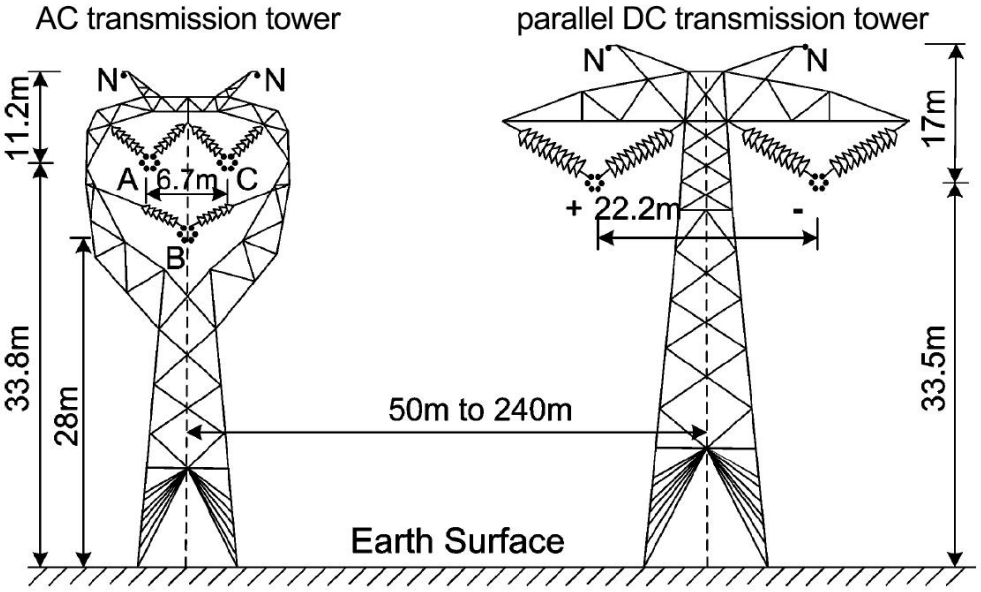

Figure (21) Figure (21) cross section diagram of parallel AC/DC transmission lines system sharing the same RoW [39].

Due to the generated transverse voltage and the induced EMF on a direct current line, EMF interference leads to a Hall effect. To calculate this, the DC component of the DC line is first obtained by calculating the total impedance. It can be seen that the induced transverse voltage is induced on both the positive and the negative DC conductor with a higher value of approximately 10 kV on the positive conductor and approximately 3 kV on the negative conductor at 50 m distance. It is observed that the induced transverse stress decreases significantly with increasing distance up to 150 m and then decreases further, but at a very slow rate. The longitudinal EMF follows the same approach as for the transverse voltage, as it is induced on both DC conductors. yet, it decreases at a lower speed and has a lower value than the transverse voltage, which reaches a maximum of about 1.5 kV on the positive DC conductor

at a distance of 50 m between AC and DC lines in case of steady state operation. As soon as a single phase to ground fault occurs on the AC lines, particularly on the phase that is closest to the DC lines, a very high current flows through the faulty AC phase, which induces a high EMF due to the inductive coupling between AC and DC lines. The induced EMF has a higher value on the positive DC conductor than on the negative one, taking the position of the DC lines into account in this model since the positive conductor is closest to the AC lines [39]. For a parallel HVAC transmission system of a voltage of 525 KV and 1 KA current in each phase alongside to HVDC lines for a parallel length of 1 Km. The resulted induced voltage on the HVDC lines are represented in the following Table (5), whereby it must be taken in consideration the positive DC conductor is closest to the AC power lines.

Table (5) results of induced voltage of a parallel HVAC/HVDC system [18]

Distance between the centers of HVAC and HVDC lines (m)	Proximately induced voltage (KV)	
	DC line +	DC line -
40 m	21 KV	8 KV
50 m	12 KV	5 KV
60 m	7 KV	3 KV
70 m	4 KV	2 KV
80 m	3 KV	2 KV

From the table above and the results, it can be seen that the induced voltage on the positive DC line over different distances is represented with higher values than on the negative one because the positive line is the closest and is therefore exposed to higher levels of electromagnetic interference. The greater the distance between the center of the HVAC and the center of the HVDC, the lower the induced voltage on both DC lines. In addition, the gap between the induced voltages on both lines becomes narrower by increasing the distance, in particular from 90 m, and keeps diminishing at steady state between them up to 140 m to approximately zero

induced voltage on both DC lines. The extent of electromagnetic coupling in parallel HVDC/HVAC systems is due to a number of factors related to line geometry and physical properties. Obviously, from the previous results, it is noticed that the distance between the parallel HVAC lines and the HVDC lines plays a major role as the electromagnetic interference can be significantly reduced and kept at a steady level by increasing the distance between the power lines of the two systems. The shorter the parallel length between the two systems, the less electromagnetic interference can occur. The rated voltage and current of the HVAC transmission lines, both induced voltage and current on the DC power lines are increased by increasing the HVAC voltage and current. The ground resistivity does not have that much influence on the electromagnetic coupling, however the arrangement of the AC lines can reduce the interference if they are arranged in a certain arrangement with the HVDC lines in the same RoW [18]. Besides, electromagnetic coupling which generates induced voltage and current on the DC lines, there is an electric field coupling as well due to parallel transmission lines of AC and DC conductors. Based on a hands-on project in northwest China, a hybrid parallel transmission system is analyzed to discuss the effects of electric field coupling on separation distance and nominal electric field (free of space charge) coupling properties on both DC and AC lines. The project consists of a 750 KV HVAC transmission system in parallel with ±800 KV HVDC transmission lines. As a result of the interaction between the two parallel systems, each system with an electric field influences the conductors of the other and vice versa. These electric fields are known as the DC electric field bias which is found on the AC lines surface due HVDC system and similarly the AC electric field bias which is present on the surface of the HVDC lines, as shown in Figure (22). Corresponding to the arrangement of the power lines in both systems, the positive DC line adjoins phase C of the AC lines, as a result of which these two conductors are exposed to a high level of interaction and thus to a higher bias value of the electrical field. It can also be noticed from Fig. (22) that AC transmission system affects with higher value of electric field bias on the DC lines.

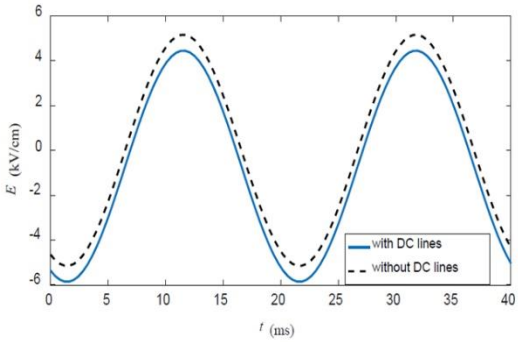

(a) DC electric field bias on phase C

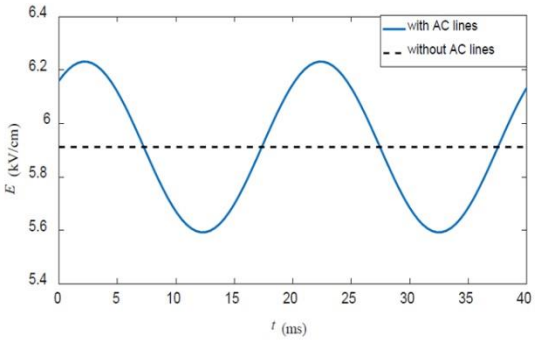

(b) AC electric field bias on positive DC line

Figure (22) the nominal coupling electric field on the surface of AC and DC lines [38].

According to the value of each electric field bias, this can affect the corona discharge of the corresponding conductor, therefore the electric field bias level is defined by the bias factor, which in turn is the ratio between the electric field bias on the conductor surface due to the adjacent parallel system to the electric field of that conductor in the absence of the parallel transmission lines. In Figure (23) the two parallel systems are displayed in mesh grid for the calculations domain using ANSYS software, representing the description for each system, where the separation distance (L) is set to 20m and the equivalent radius is obtained for both AC and DC lines as r_1 and r_2 respectively.

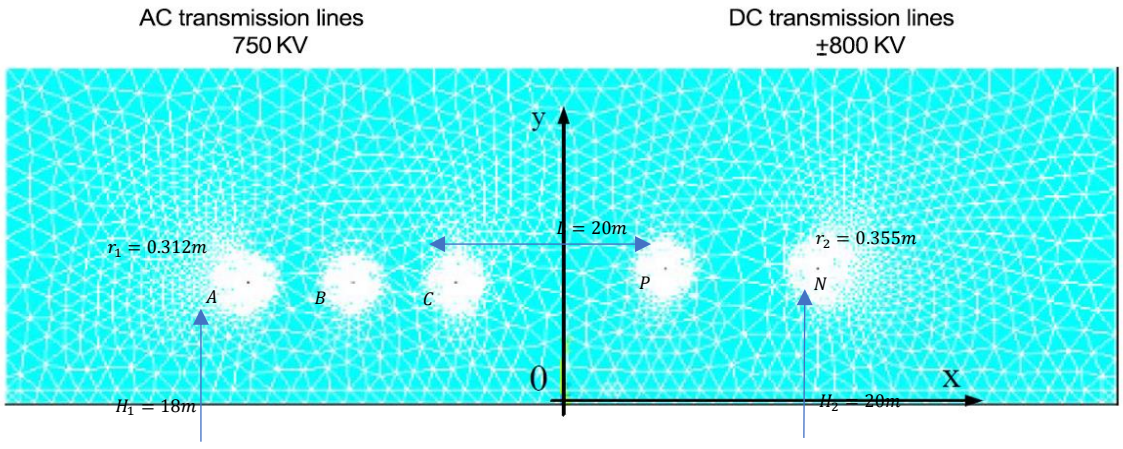

Figure (23) mesh grid of calculation area for a hybrid parallel HVDC and HVAC transmission lines [38].

After the electric fields (E) are calculated on the surface of each conductor for AC and DC lines by following some procedures with the help of finite element method (FEM) and finite volume method (FVM) to solve the equations, the electric field bias factors can be obtained for each conductor using the following equations:

$$\delta_{AC} = \frac{E_{bDC}}{E_{nAC}} \times 100\% \quad (6)$$

Similarly

$$\delta_{DC} = \frac{E_{bAC}}{E_{nDC}} \times 100\% \quad (7)$$

Where δ_{AC} and δ_{DC} are the electric field bias factors for AC and DC lines, respectively, E_{bDC} and E_{bAC} are the bias DC electric field on the AC conductor and the bias AC electric field on the DC conductor, respectively, E_{nAC} and E_{nDC} are the nominal AC electric field without the influence of DC transmission lines and the nominal DC electric field without the presence of AC electric fields, respectively. The results show that as the distance between the AC and DC lines increases, the bias factors decrease. Because phase C of AC power lines and the positive DC conductor are closest from either side, they have the highest bias factor of 5.4% for AC phase C and 6.9% for positive DC conductor. On the other hand, the most distant conductors of each system have smaller percentage biasing factors since the negative DC line is 1.3% and the phase A of the AC lines is 0.28%. It can be seen that AC power lines have an impact with higher electric fields on DC power lines than those on AC power lines due to the parallel DC transmission system. The calculations are repeated for various separation distances, and from results it can be seen that the greater the distance between the two parallel systems, the less the interaction between them and therefore smaller bias factors. If L is set to 30 m or more for this project, then the electric field coupling and interaction between AC and DC lines can be neglected with AC phase C and positive DC conductor bias factors of 2.7% and 3.5% at 30 m, respectively [38]. Insights into the results from [45] show that the various types of power transmission lines sharing the same tower influence each other through space charges and the total electric field, which is the sum of the AC electric field, DC electrostatic field and electric field due to space charges. The results are based on a project carried out in China of 1000 kV HVDC transmission lines Mengxi-Tianjinnan and a bipolar ±800 kV HVDC transmission system Zhalute-Qingzhou, from which all parameters are taken. The results are taken for different models with overlay HVDC-HVAC hybrid system, with different results of the electrical coupling

field being displayed in each model by changing the position of both systems above and below each other and by changing the arrangement of the power lines either horizontally or vertically.

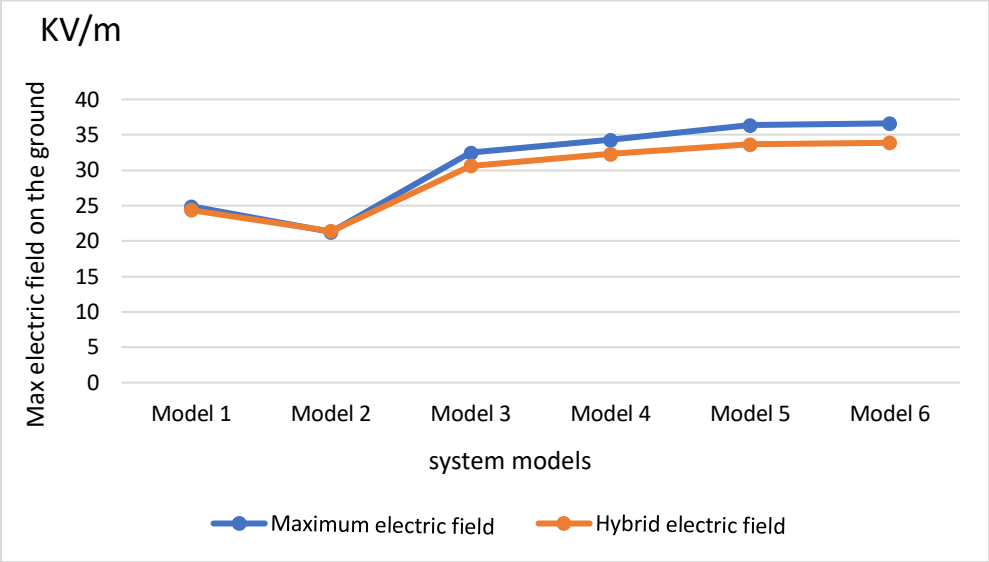

Figure (24) comparison chart results of maximum and hybrid electric fields on the ground for different models [ibid.]

As can be seen from the results in Figure (24), results of the maximum and hybrid electric fields in Model 1 and Model 2 differ only slightly, with both DC power lines lying above the AC power lines. However, in model 1 the AC power lines are in a horizontal plane and in a triangular position in model 2 with a vertical distance between the two types of 10 m. Model 5 and Model 6, where the results gap tends to be slightly larger than in the previous models, the power lines of HVDC and HVAC systems are arranged in a vertical plane. The transmission lines in Model 5 are side by side in a parallel position on the same tower. However, on Model 6, the AC power lines are in a vertical double circle above the horizontal DC power lines. These different results suggest that the electrical coupling field of a hybrid HVAC-HVDC transmission system on the same RoW relies on various factors which are the relative position of the phase arrangement of AC power lines and DC power lines, the line parameters, and the number of AC circuits.

8 Sizing DC power transmission lines

The first step and the main dominant in designing an HVDC transmission system depends on the estimated amount of energy that needs to be transmitted, as well as some other factors

such as the distance from the source to the loads, environmental specifications, corona losses, voltage drop, and power losses. Since the determination of the mount of the transmitted energy can recognize which type of DC link is suitable, whether monopolar or bipolar, and shows the conductor qualifications and dimensions. This is followed by the location of the sending and receiving power converter stations. As a rule, the sending units are located in the vicinity of the power generation location. However, the receiving units depend mainly on the economic evaluation of the project. The evaluation of the conductor size relies on the amount of power transmitted and the rated current flowing through it. In practice, the transmitted power and rated current value are determined, so there is always the possibility of using different types of conductors suitable for the specified values of power and current. Therefore, some calculations, for instance, the value of the corona losses, voltage drops across the conductor, and Joule losses, are then performed to compare these options and based on the results the best suitable conductor type is chosen [2]. For any transmission system, there are only two types either to be overhead lines or underground conductors. Overhead lines are preferred when possible to reduce costs and simplify maintenance. They are also made of aluminum due its light weight and lower cost as well. There are four types of aluminum conductors which are: all-aluminum alloy-conductor (AAAC), all-aluminum-conductor (AAC), aluminum-conductor-steel-reinforced (ACSR) and aluminum-conductor-alloy-reinforced (ACAR). The ACSR type is the most widely used among them as it is made from several alternating layers of stranded aluminum conductors wound around the stranded steel core to increase strength with the conductor weight and in the opposite direction to hold the strands together and to increase flexibility. Moreover, the conductors are arranged in a bundle configuration, which means that, especially in high voltage transmission systems, an additional conductor or more per pole are used to reduce corona losses and increase current capacity. The corona discharge depends on the conductor configuration, conductor diameter, surface condition and weather conditions. By increasing the number of conductors per pole, the total cross-sectional area increases and the resistance decreases. Figure (25) shows some typical examples of stranded conductor arrangements in different bundle configurations. Typically, such configurations are used for transmission systems from 345 kV to provide a high current capacity for each line and to limit the corona effect. Spacers are steel or aluminum rods used to maintain the distance (d) between the conductors of each pole [21].

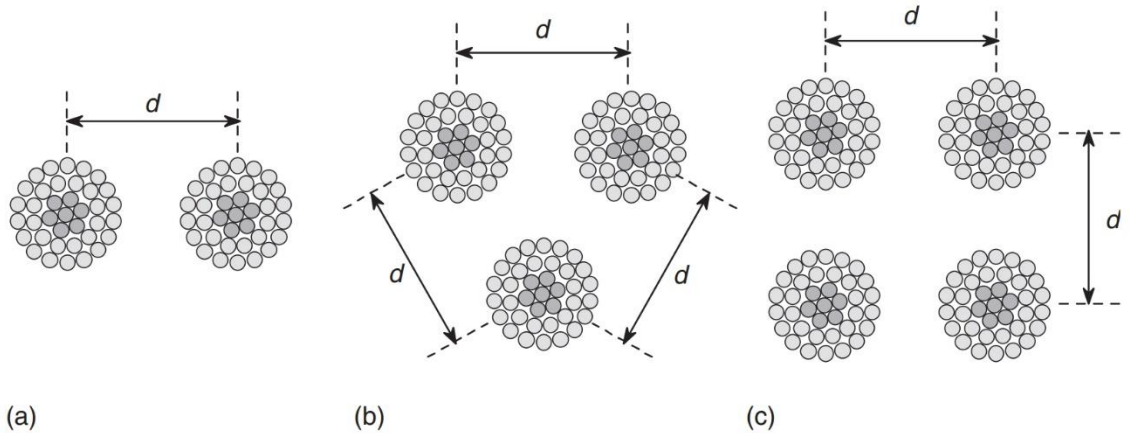

Figure (25) models of typical configurations for bundle stranded conductors per pole of (a) double, (b) triple, and (c) quadrupole [ibid.].

8.1 Analyzed case study

In general, when designing an HVDC transmission system, three aspects are considered from the cable point of view: the cable material itself including cable specifications and insulation material, the cable joints and the cable terminations. For cables, the most widely used technology for high power DC cable implementations, that has been developed over time since its first application in the late 1990s, is extruded cables surrounded by cross-linked polyethylene XLPE as an insulation material. This technology offers some advantages such as simplicity in the production and installation process, environmentally friendly properties, less maintenance and lower weight. The extruded XLPE HVDC cables have the ability to keep space charge under control to prevent electrical failure or breakdown of the cables. The cable joints are intended to connect between two extruded cables and consist of two types, the fabricated joints and the pre-fabricated joints. The fabricated joints are made between two cable sections by welding their cable conductors and applying the same material of insulation layers and semiconductors of the actual cables which leads to similar mechanical properties as the cables. However, this process requires a high level of cleanliness, long time and good control during installation. In contrast, the prefabricated joints do not require a long installation time since they are firstly pre-molded and then installed on site by sliding the joint body onto the two cable sections. The cable terminators are designed to support the cable to withstand voltage

transients and keep the DC electrical field sufficiently uniform. The corona ring can be adapted to it according to the environment needs [12].

A study case is being analyzed to replace a 400 kV HVAC transmission system with an HVDC transmission system in Turkey that connects the south-eastern part of Turkey in Keban, where the power generation and sending units are, with the western part of the country in Adapazari. The transmitted power generated by hydropower stations in Keban is 3000 MW and on this basis a bipolar system is chosen. The distance between the sending and receiving points is approx. 1000 km and therefore the ground is used as a return path as an alternative to a metallic return conductor. Depending on the power capacity, each pole should deliver 1500 MW. Based on the voltage level standards of the HVDC system and the actual HVAC voltage level, two HVDC systems with ± 500 kV and ± 600 kV are selected for comparison. Figure (26) describes a 2D RoW sketch of the tower dimensions and geometry.

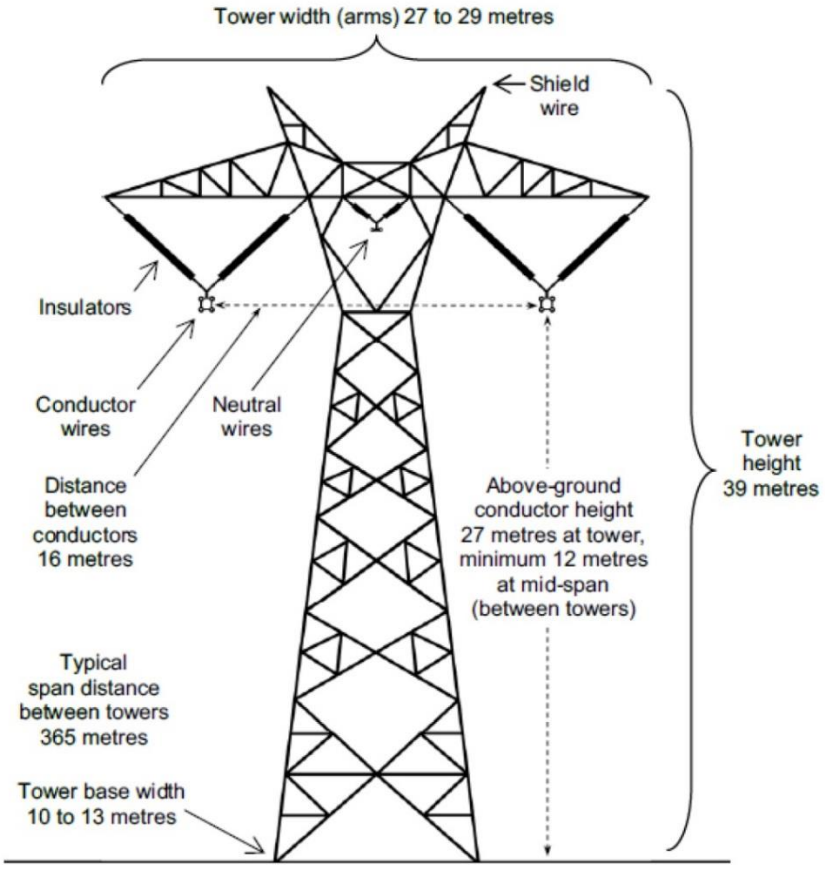

Figure (26)HVDC transmission tower dimensions and geometry [2].

After defining the DC link type, which is a bipolar, the next step is to select the conductor size by determining the current flows in each pole and the power delivered. For an HVDC system with ± 500 kV and a total of 3000 MW, the current in each pole is:

$$I = \frac{S_{max}/2}{U} = \frac{3000 \times 10^3}{2 \times 500} = 3000\ A \quad (8)$$

Similarly, for ± 600 KV transmission system,

$$I = \frac{3000 \times 10^3}{2 \times 600} = 2500\ A$$

Then two conductor types are suggested, 1272 MCM BITTERN conductor type for the option of 2500 A and ±600, the other one is 954 MCM RAIL conductor type for the option of 3000 A and ± 500 KV, Figure (27) shows the specifications for both of them [2].

ELAND CABLES

CODE	SIZE KCM	STRANDING No. x mm		SECTION mm²		OVERALL DIAMETER mm		CONDUCTOR WEIGHT kg/km			RATED STRENGTH kN	ELECTRICAL RESISTANCE			CURRENT CARRYING CAPACITY Amps
		Al.	Steel	total	Al	Total	Core	Total	Al.	Steel		20°C DC	25°C AC	75°C AC	
CONDOR	795	54 x 3.08	7 x 3.08	454.5	402.3	27.72	9.24	1513.9	1116.1	407.8	125.48	0.07054	0.07283	0.08694	975
MALLARD	795	30 x 4.14	19 x 2.48	495.6	403.8	28.96	12.4	1837.9	1118.7	719.2	170.87	0.06988	0.07218	0.08596	1005
RUDDY	900	45 x 3.59	7 x 2.40	487.2	455.5	28.74	7.2	1510.5	1263.5	247	108.58	0.06234	0.06463	0.07743	1050
CANARY	900	54 x 3.28	7 x 3.28	515.4	456.3	29.52	9.84	1724.8	1263.5	461.3	141.95	0.06234	0.06463	0.07710	1055
CATBIRD	954	36 x 4.14	1 x 4.14	498.1	484.6	28.98	4.14	1437.6	1333.4	104.2	88.11	0.05971	0.06234	0.07415	1095
RAIL	954	45 x 3.70	7 x 2.47	517.3	483.8	29.61	7.41	1599.8	1339.4	260.4	115.25	0.05938	0.06201	0.07382	1090
CARDINAL	954	54 x 3.38	7 x 3.38	547.3	484.5	30.42	10.14	1829	1339.8	489.2	150.4	0.05906	0.06135	0.07316	1095
TANAGER	1033.5	36 x 4.30	1 x 4.30	537.3	522.8	30.1	4.3	1556.6	1433.5	113.1	95.23	0.05577	0.05873	0.06923	1130
ORTOLAN	1033.5	45 x 3.85	7 x 2.57	560.2	523.9	30.81	7.71	1733.7	1451	282.7	123.26	0.05479	0.05741	0.06824	1150
CURLEVV	1033.5	54 x 3.52	7 x 3.52	593.6	525.5	31.68	10.56	1980.8	1451	529	162.86	0.05446	0.05677	0.06759	1150
BLUEJAY	1113	45 x 4.00	7 x 2.66	604.4	565.5	31.98	7.98	1867.7	1562.6	305.1	132.6	0.05085	0.05348	0.06365	1205
FINCH	1113	54 x 3.65	19 x 2.19	636.6	565	32.85	10.95	2129.6	1570	559.6	174	0.05085	0.05315	0.06332	1205
BUNTING	1192.5	45 x 4.14	7 x 2.76	647.7	605.8	33.12	8.28	2000.1	1674.2	325.9	142.4	0.04757	0.0502	0.05938	1255
GRACKLE	1192.5	54 x 3.77	19 x 2.27	679.7	602.8	33.97	11.35	2281.4	1681.7	599.8	186.45	0.04724	0.04954	0.05906	1260
SKYLARK	1272	36 x 4.78	1 x 4.78	664	646	33.46	4.78	1916.8	1776.9	139.9	117.48	0.04462	0.04757	0.05643	1310
BITTERN	1272	45 x 4.27	7 x 2.85	489.1	644.4	34.17	8.55	2134.1	1785.8	384.3	151.74	0.04462	0.04724	0.0561	1310
PHEASANT	1272	54 x 3.90	19 x 2.34	726.8	645.1	35.1	11.7	2423.5	1783.8	639.7	199.96	0.04429	0.04659	0.05545	1310
DIPPERF	1351.5	45 x 4.40	7 x 2.93	731.4	684.2	35.19	8.79	2266.5	1898.5	368	161.08	0.04199	0.04495	0.05282	1360
MARTIN	1351.5	54 x 4.02	19 x 2.41	772.1	685.4	36.17	12.05	2585	1906.4	678.6	206.03	0.04167	0.04396	0.05217	1365
BOBOLINK	1431	45 x 4.53	7 x 3.02	775.4	725.3	36.24	9.06	2400.4	2009.1	391.3	170.43	0.0397	0.04265	0.0502	1410
PLOVER	1431	54 x 4.14	19 x 2.48	818.7	726.9	37.24	12.4	2738.3	2019	719.3	218.48	0.03937	0.04167	0.04954	1415

Figure (27) standard codes of ACSR conductors alongside with their technical specifications [50].

The suggested bundle pole configurations are 4x1272 MCM, 3x1272 MCM and 3x954 MCM with a 7-stranded shielding wire of 9.5 mm2. Some calculations are then done to evaluate these alternative options and choose the best one. In this study, hourly Joule losses for each configuration are determined with the help of the daily load profile and the average value is used for comparison. Afterwards, corona losses with voltage drop are calculated. The results show that all three proposed configurations are suitable for designing this HVDC transmission system. Even though each configuration shows better results than the other ones in each calculation, yet most importance with line losses in which 4x1272 MCM for ± 600 KV show the lowest losses among them and for voltage drop values are obviously low, since the DC link is only used for transmitting power and not for feeding loads [2].

8.2 Calculated case study

A. Overview and theories

The maximum current carrying capacity flowing through a cable is known as the cable ampacity, which is considered to be the main factor in determining the size of the cable conductor. Alongside heat dissipation factor and including some other factors such as, steady state, transient, and short circuit values. Heat dissipation describes the amount of inner heat that the conductor is able to dissipate through the insulation material to the surroundings, and therefore depends on the conductivity of the insulation and environment conditions. Obviously, the risk of partial damage to the cable or a complete failure increases by increasing the operating load current, which in turn leads to a higher operating temperature in the cable and can damage the insulation layer, in particular over long distances. For this aim to avoid any failure, the cable ampacity is measured for a de-rated value which is a much less than the actual maximum ampacity and defined as the de-rated ampacity [9]. Moreover, with buried submarine cables, more factors affect the cable ampacity and take into account considerations such as: burial depth, the distance between the cables. In other words, the heat dissipation criteria define the cable ampacity and the installation ability to extract this heat due to the high current flow into the surrounding medium. The conduction heat, which is derived according to Fourier's law and indicates the heat flow transferred by conduction, is proportional to the ratio of temperature to space. Convective heat is found in moving fluids such as water and air, dependent on temperature differences and subject to Newton's law. And the last is heat caused by radiation which follows Stefan-Boltzmann Law and is proportional to the heat difference at the power of

four. Compared to AC cables the heat generated is presented in both conductors and insulators and mainly related to power frequency which in case of power DC cables becomes zero once the DC voltage is applied and therefore the heat source in DC cables exists only in conductors [22]. Another parameter plays an important role in the design of HVDC cables. The calculations of the electrical field distribution depend on the applied voltage, the cable geometry and the electrical conductivity of the insulation layers as well. As soon as the cable runs under load, a thermal gradient occurs in the insulation layers which, due to the higher electrical conductivity, leads to a space charge accumulation and causes a field inversion or a modified electrical field. This indicates that the maximum temperature difference across the insulation, which is approved by the manufacturer, is one of the main parameters when selecting and designing HVDC cables in order to keep the electric field strength below the breakdown limit according to the medium. By switching the operating voltage by means of capacitive control to the unloaded cold cable with almost uniform electrical conductivity of all insulation layers, a thermal gradient occurs. Depending on the applied voltage and cable geometry as a function of the radial radius of the cable center, the field strengths $E(r)$ at the inner edge of the insulation (r_i), where the field strength is maximum, and at the outer radius of the insulation (r_o) are derived from Laplace's field strength equation as follows:

$$E(r) = \frac{U_0}{r \ln\left({}^{r_o}/_{r_i}\right)} \tag{9}$$

Where $r = r_i$ to measure the maximum electric strength at the inner border of the insulation, and $r = r_o$ to measure the field strength at the insulation surface. Due to operating voltages and pulse voltages, which lead to two minimum thicknesses of the insulation layer, there are two values for E_{max} and then the thicker one is selected according to formula (10) as follows [6]:

$$S_{min} = r_i \left[e^{{}^{U_0}/_{(r_i E_{max})}} - 1 \right] \tag{10}$$

The cable ampacity is calculated using the Neher-McGarth method by dividing the cable layers based on their thermal resistance. Figure (28) shows the different layers of a typical submarine DC cable construction.

Construction:

1 -Conductor (key-stone type)
2 -Conductor shielding
3 -Insulation (mass-impregnated paper)
4 -Insulation shielding
5 -Lead sheath
6 -Plastic jacket
7 -Tape armor bedding
8 -Optical fiber
9 -Steel wire armor
10 -Serving

Figure (28) construction layers for a typical submarine DC power cable [22].

The heat transfer in a DC cable through its layers is shown in Figure (29) as a thermoelectric equivalent circuit diagram. The temperature difference between the circuit terminals of the rising heat via the inner core conductor (K_c) in relation to the ambient temperature (K_{amb}) is represented as the potential difference (ΔK). Whereas these heat sources describe the electrical losses that are only present in conductors and are defined by Joule losses (W_c), they can be computed according to expression (11).

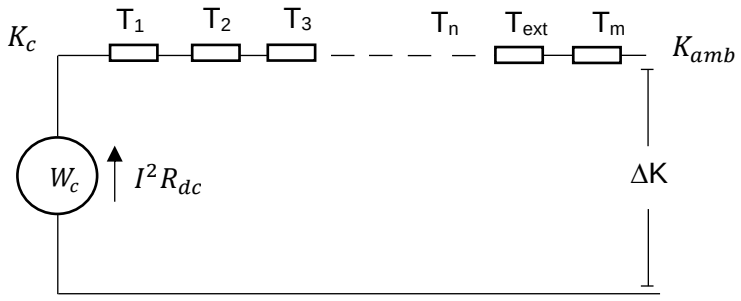

Figure (29) thermoelectric equivalent circuit diagram of heat transfer in a DC power cable [ibid.].

Where:

$$W_c = I^2 R_{dc} \tag{11}$$

$$\Delta K = K_c - K_{amb} = W_c \left(T_1 + T_2 + T_3 + \cdots + T_n + T_{ext} + T_m \right) \tag{12}$$

From expressions (11) and (12), the cable ampacity can be computed as:

$$I = \sqrt{\frac{K_c - K_{amb}}{R_{dc} \left(T_1 + T_2 + T_3 + \cdots + T_n + T_{ext} + T_m \right)}} \tag{13}$$

Where: T_n is the thermal resistance according to layer sequence, T_{ext} is the external medium thermal resistance after the cable materials and T_m is the mutual thermal resistance. The accurate calculations of the DC resistance and thermal resistances of each layer are important in sizing the cable and determining the ampacity rating of it [22]. Further equations for the exact calculation of the thermal resistance of cable layers, the external thermal resistance and the mutual thermal resistance are expressed in [ibid.]. Since the voltage and current of HVDC cables are stationary, the magnetic fields generated by DC cables are static fields as opposed to those from AC cables, where the current alternates, and AC magnetic fields can induce currents or voltages in nearby objects. Due to the thin insulating layers and the steel wire armor that surround the core conductor of the HVDC submarine or the underground cable, they have a higher capacity than overhead lines. Cable capacitance increases with cable length and is charged when the voltage level changes or when the cable is first energized. However, there is no additional current required as in case of AC cable that is needed to charge AC cable capacitance, there is still some current loss through the dielectric insulator of DC cables, but it is relatively small compared to the actual cable current level, and the DC cables are limited only by their heat transfer rate and conduction loss. The magnitude of both the magnetic field strength H and the magnetic flux density B of a DC cable tends to be the maximum at the surface between the core conductor and the insulation layer if there are no additional influences for the magnetic field. Then after reaching the highest value of both B and H, they begin to decay in non-linear curves in the insulation area with increasing distance. If a steel armor layer with a higher magnetic permeability (μ) is added, this affects the distribution behavior of H and B, especially the magnetic flux density B, which reaches large value at some point in the insulation layer, besides an obvious growth of H in the armor layer. Nevertheless, the overall magnetic field strength is low and has no harmful effects on the cable or the surroundings. In the case of double or triple-core cables, the magnetic field density is greater in a triple type since the magnetic field is superimposed, and in both types, it has lower values in the middle area

between the conductors and higher values near the conductors. The previous part can be applied to discuss the behavior of B and H in a practical submarine cable with return cable that is widely used due to the bipolarity of the current flowing. The magnetic field strength is similarly distributed so that it has the highest values around the conductors. On the other hand, B in the steel layer becomes relatively high due to its higher μ compared to other cable materials. The relation between magnetic field strength H and flux density B can be defined by (14):

$$B = \mu . H \tag{14}$$

Where μ is a changeable parameter related to the permeability of the material, B is the magnetic flux density defined by the unit of Tesla (T) and H is the magnetic field strength defined by Amps/meter (A/m) [46].

B. Background and calculations

The hydropower plant of Itaipu has a HVDC transmission system which is a connection project between Paraguay and Brazil. It is designed to transmit a total power of 12,600 MW from Itaipu to Southeastern in Brazil. Due to the country frequency contrast between 50 Hz and 60 Hz, half of the power is transmitted from a 6,300 MW 765 KV HVAC system and the other half from a HVDC link, which is represented in two bipolar transmission systems with a rated voltage of ± 600 KV as shown in Figure (30). The rated voltage ± 600 kV is chosen as the optimal voltage for best performance and economic aspect. The two bipolar DC links are designed so that they work independently of one another. This has the advantage that in case of fault occurs on one of them, the other one is still in operation and can deliver half the power capacity. The two bipolar transmission lines are built over a distance of approximately 800 km with a RoW spacing of at least 10 km apart [28].

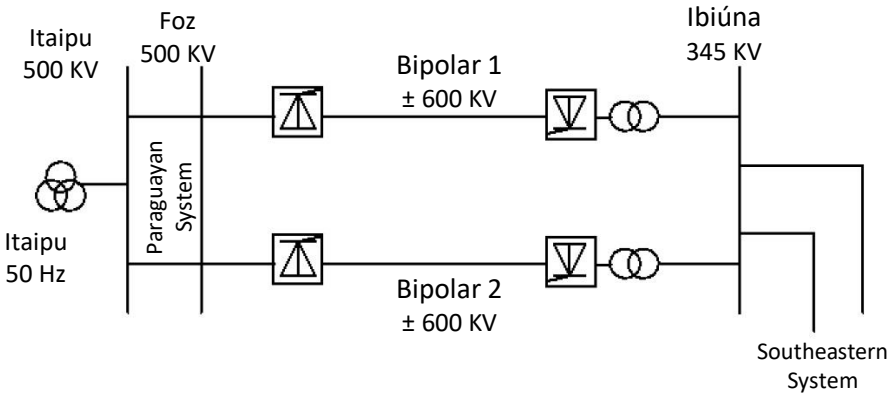

Figure (30) simplified diagram of the 6300 MW ± 600 KV Itaipu transmission system [ibid.].

Each bipolar delivers a power of 3150 MW and has no metallic return line, so ground is used as the return path and for maintenance purposes or pole outage nowadays. Each pole of bipolar lines is connected to two converters and one earth electrode with a corresponding electrode line. The electrodes are buried about three meters deep and conventionally structured as a ring of silicon iron rods that are embedded in a layer of coke. The choice of ± 600 kV as the optimal line voltage has proven to give a good experience over the years. This can be seen from the fact that the average failure rate per 100 km / year is actually less than one failure. With these faults in mind, they are related to pole faults and 20% of them require an operator action to restore it, while a bipolar failure is just a case of mechanical failure of the tower [14].

For one 3150 MW ± 600 KV Bipolar link:

The current flows in each pole is computed as:

$$I = \frac{S_{max}}{2 \ * \ U} = \frac{3150 * 10^3}{2 * 600} = 2625 \ A$$

Where is S_{max} the maximum transmitted power of a pole and U is the rated line voltage.

Based on the flowing current of each pole, the two suggested conductor configurations that are constructed in four bundle arrangements and with the help of Figure (28) are 4xBUNTING 1192.5 MCM 606 mm^2 45/7ACSR and 4XBITTERN 1272 MCM 644 mm^2 45/7ACSR. These configurations are proposed based on the fact that the current in the conductor is selected according to the de-rated value previously discussed in point A, therefore the two bipolar transmission systems operate independently of one another and in the event of a complete outage of one bipolar line, the other can still be operating and supplying total power.

Then due to four bundle configuration, the current in each sub-conductor is:

$$I_{sub} = \frac{I}{4} = \frac{2625}{4} = 656.25\ A$$

Joule losses can be computed for both conductor types from:

$$P_{total,losses} = I_{sub}^2 * Max.DC\ resistance\ at\ 20°C\ \Omega\ /\text{km}\ \ * 4$$

For BUNTING 1192.5 MCM conductor type and 800 Km distance for two poles:

$$P_{total,losses} = 656.25^2 * 4 * 0.047 * 800 * 2 = 129.5\ \text{MW}$$

Similarly, for BITTERN 1272 MCM conductor type:

$$P_{total,losses} = 656.25^2 * 4 * 0.044 * 800 * 2 = 121.3\ MW$$

The daily hourly load profile is needed to calculate the total Joule losses over the day according to the required load. Due to the lack of the required load profile date for this project, an assumption is made based on the average hourly load profile of the northeast in Brazil from [27], by multiplying the approximate values of a typical summer day in this case by the load factor (0.7) to match the peak value of the demanded load for this project. Through some research it has also been found that both the northeast and southeast have a similar load profile regardless of the value of the required load. Therefore, this assumption can be applied in this case. Then the average hourly load profile can be seen in the following Figure (31). Following the previous guidelines to calculate the Joule losses for each conductor with respect to the demanded load for each hour of the day. Table (6) shows the results, which indicate the values of Joule losses for both conductor types according to daily hour load. It can be observed that the 4XBITTERN 1272 MCM conductor configuration has an average Joule losses value of 83.4 MW, which is less than that of the 4xBUNTING 1192.5 MCM of 89.1 MW. These results show that for 4xBITTERN 1272 MCM the choice of conductor is better from the point of line losses in the conductor.

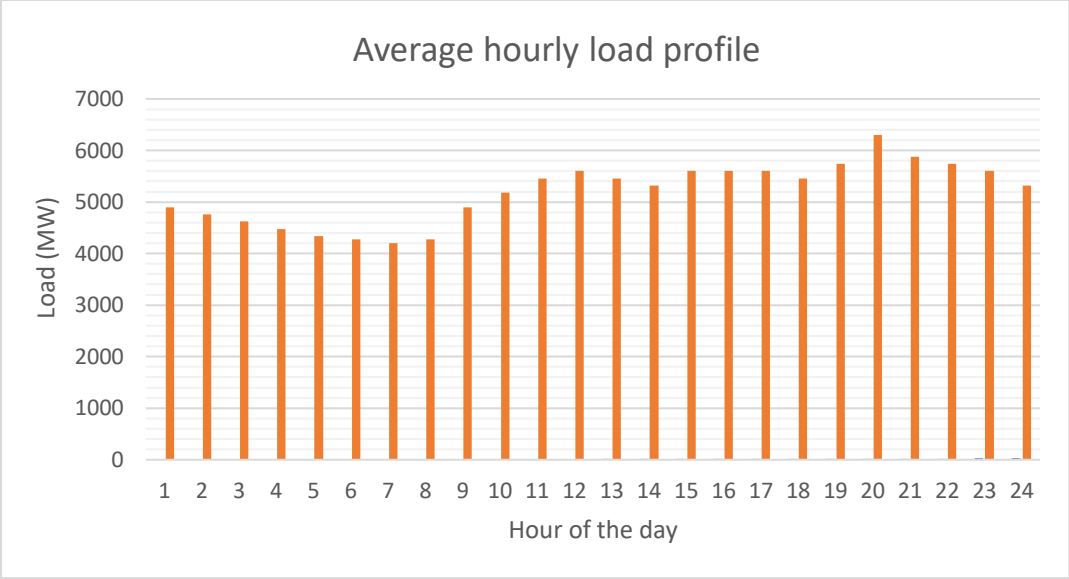

Figure (31) approximate assumption of average hourly load profile of a summer day in SE in Brazil

Line resistive (Joule) losses are considered to be the most dominant scale of line loss variables when comparing losses resulting from the transmission of bulk power over HVDC lines. Other losses are clearly important to technical considerations and the design of the system, such as, corona losses and voltage drops along the length of the line. Insight into the results in [2], it can be observed that the corona losses are far less than the Joule losses in magnitude. The same scenario applies to voltage drop, which is an important factor and needs to be calculated for transmission systems and for an HVDC lines the values are acceptable. The magnetic field resulting from a DC power line has a constant orientation and in the vicinity of its RoW the magnitude of the magnetic flux density has closer values to that of the earth's magnetic field density. In general, the magnitude of the magnetic fields depends mainly on the rated current flowing in a DC conductor and the distance far from it. For the Itaipu project, the xBITTERN 644mm2 45/7ACSR conductor was the actual conductor used in the transmission lines over a distance of 792 km for bipolar line 1 and 820 km for bipolar line 2. According to the rated voltage of the line ± 600 Kv four-bundle configuration was used with a separation sub-conductor distance of 450 mm and a distance between the poles of 16,40 meters [14].

Table (6) results of hourly line losses of the two conductor configurations with the average hourly value

Daily hours	Load (MW)	Conductor current	Sub-conductor current	BUNTING Joule losses (W)	BITTERN Joule losses (W)
1	4900	2041,67	510,42	78,4E+6	73,4E+6
2	4760	1983,33	495,83	74,0E+6	69,2E+6
3	4620	1925,00	481,25	69,7E+6	65,2E+6
4	4480	1866,67	466,67	65,5E+6	61,3E+6
5	4340	1808,33	452,08	61,5E+6	57,6E+6
6	4270	1779,17	444,79	59,5E+6	55,7E+6
7	4200	1750,00	437,50	57,6E+6	53,9E+6
8	4270	1779,17	444,79	59,5E+6	55,7E+6
9	4900	2041,67	510,42	78,4E+6	73,4E+6
10	5180	2158,33	539,58	87,6E+6	82,0E+6
11	5460	2275,00	568,75	97,3E+6	91,1E+6
12	5600	2333,33	583,33	102,4E+6	95,8E+6
13	5460	2275,00	568,75	97,3E+6	91,1E+6
14	5320	2216,67	554,17	92,4E+6	86,5E+6
15	5600	2333,33	583,33	102,4E+6	95,8E+6
16	5600	2333,33	583,33	102,4E+6	95,8E+6
17	5600	2333,33	583,33	102,4E+6	95,8E+6
18	5460	2275,00	568,75	97,3E+6	91,1E+6
19	5740	2391,67	597,92	107,5E+6	100,7E+6
20	6300	2625,00	656,25	129,5E+6	121,3E+6
21	5880	2450,00	612,50	112,8E+6	105,6E+6
22	5740	2391,67	597,92	107,5E+6	100,7E+6
23	5600	2333,33	583,33	102,4E+6	95,8E+6
24	5320	2216,67	554,17	92,4E+6	86,5E+6
				average losses Value (W)	average losses Value (W)
				89,1E+6	83,4E+6

9 Conclusion

In this thesis the comparison between HVAC and HVDC transmission systems is discussed from the point of view of economic evaluation, technical aspects and environmental impacts. HVDC transmission lines have been shown to perform better economically than AC lines when the transmission route crosses the breakeven point that ranges from 400 to 700 km for overhead lines and 50 km for submarine cables. This emerges from the supported results of practical projects that show the economic superiority of HVDC lines for transmitting bulk power over long distances. Long-distance DC transmission line shows a higher hand than AC lines in some technical respects, demonstrating the ability to transmit higher power with less line losses, faster control interruption in the event of faults, and better system stability.

The implementation of HVDC transmission system can be done through two technologies, the current source converter (CSC) based HVDC and the voltage source converter (VSC) HVDC system. They differ in the operating voltage, since CSC-based HVDC systems can be operated with higher rated voltages up to 1000 KV and thus transmit higher power. These two technologies are viewed as part of the overall HVDC transmission system, demonstrated as a part of the converter station that includes the converter transformer, capacitor sets, etc. The DC link corresponding to the desired power to be transmitted, the rated line voltage voltage, is thus selected with the DC link type, which can be a monopolar, bipolar or homopolar connection.

With the help of power electronic devices such as power diodes, different types of power thyristors and IGBTs that are discussed as well in this paper, various topologies of HVDC transmission systems are introduced for different applications. Varying from monopolar and bipolar systems to multi-terminal applications that are very suitable for renewable energy projects in particular for the integration of offshore wind farms into AC networks through different topologies. The wind farm ring topology is characterized by adding more flexibility in case of fault occurs and precise control of the power flow. The HVDC transmission system offers some advantages and is therefore very well suited for various applications. It can be used to establish a connection between two AC networks with different operating frequencies via asynchronous DC ties. The best HVDC technology with weak AC grid connections is the VSC-based HVDC due to its quick recovery capability without commutation failure. Best suited for long distance bulk power transmission and the very distant, remote areas such as various loads on islands with high reliability thanks to VSC-based HVDC technology.

The extruded cables with cross-linked polyethylene (XLPE) insulation material are the commonly type used for HVDC transmission lines. The degassing process is applied during manufacturing to keep the by-product level down and avoid the accumulation of space charges during operation and degradation of the material to breakdown. A modified electro-acoustic pulse system (PEA) is explained to measure and investigate the behavior of the space charge distribution of a cable sample exposed to an HVDC source. After experimental discussion of the degassing process over different time intervals, it is found to be efficient and effective when applied for a certain time to improve the local distribution of the electric field. The mean potential difference between any two points within the enclosed radial area of a conductor carrying DC is proportional to the square of the current flowing through the conductor. In the case of high temperature superconducting DC cables (HTS), the uniformity of the critical current distribution over all tapes is required to avoid possible damage to the cable. Hybrid HVDC-HVAC transmission systems with the same RoW result in electromagnetic coupling due to the mutual capacitance and inductance between them. As a result, an induced EMF on DC lines is presented with a higher value at the pole closest to AC lines and causes a transverse voltage. The greater the distance between the center of the HVAC and the center of the HVDC, the lower the induced voltage on both DC lines. In addition to the electrical coupling field in the hybrid system, it relies on various factors which are the relative position of the phase arrangement of AC lines and DC lines, the line parameters, and the number of AC circuits.

The sizing of a DC transmission line depends on the desired amount of transmitted power, the distance and the rated voltage of the line. Bundle conductor configurations are used for transmission systems from 345 kV to provide a high current capacity for each line and to limit the corona effect. The amount of power transmitted defines the appropriate corresponding rated voltage to reduce losses and costs, the type of DC link is then selected. This in turn defines the cable ampacity, which determines the conductor size, taking into account different losses in the conductor, for instance, Joule losses, voltage drops and corona losses. Network fault considerations are essential and so conductor sizing is based on the de-rated value. The heat dissipation of a cable describes the electrical losses that are only present in the core conductor. The thermal resistance of each layer is important to define the cable ampacity. The magnetic fields generated by DC cables are static fields as opposed to those generated by AC cables. A case study is introducing based on the selection for the DC transmission line and sizing it.

10 References

[1] Aredes, M., Aquino, A. F. C., and Santos Jr, G. 2001. Multipulse converters and controls for HVDC and FACTS systems. *Electrical Engineering (Archiv fur Elektrotechnik)* 83, 3, 137–145.

[2] Aytug Font, Suat Ilhan, Hasbi Ismailoglu, Fermin Espino Cortes, and Aydogan Ozdemir. *Design and Technical Analysis of 500-600 kV HVDC Transmission System for Turkey*. http://www.eleco.org.tr/openconf_2017/modules/request.php?module=oc_proceedings&action=view.php&id=305&file=1/305.pdf&a=Accept+as+Lecture.

[3] Bahrman, M. P. *Overview of HVDC transmission*.

[4] Bahrman, M. P. 2008. HVDC transmission overview. In *IEEE/PES Transmission and Distribution Conference and Exposition, 2008*. *T & D ; 21-24 April 2008, [Chicago, IL]*. IEEE, Piscataway, NJ, 1–7. DOI=10.1109/TDC.2008.4517304.

[5] Baliga, B. J. 2019. *Fundamentals of Power Semiconductor Devices*. Springer International Publishing, Cham.

[6] Brakelmann, H. and Anders, G. J. 2018. Current Rating Considerations in Designing HVDC Cable Installations. *IEEE Trans. Power Delivery* 33, 5, 2315–2323.

[7] D.M. Larruskain, I. Zamora, A.J. Mazon, O. Abarrategui, J.Monasterio. Transmisson and Distribution Networks: AC versus DC.

[8] Dennis A. Woodford. 1998. *Basis principle of HVDC*. *HVDC transmission*.

[9] Duraisamy, N. and Ukil, A. 10/25/2016 - 10/27/2016. Cable ampacity calculation and analysis for power flow optimization. In *2016 Asian Conference on Energy, Power and Transportation Electrification (ACEPT)*. IEEE, 1–5. DOI=10.1109/ACEPT.2016.7811535.

[10] Electrical4U. 2019. *Surge Impedance Loading or SIL | Electrical4U*. https://www.electrical4u.com/surge-impedance-loading-or-sil/. Accessed 13 December 2019.

[11] Electrical4U. 2020. *Switching or ON OFF Characteristics of SCR or Thyristor | Electrical4U*. https://www.electrical4u.com/switching-of-on-off-characteristics-of-scr-turn-on-turn-off-time/. Accessed 8 February 2020.

[12] Ghorbani, H., Jeroense, M., Olsson, C.-O., and Saltzer, M. 2014. HVDC Cable Systems—Highlighting Extruded Technology. *IEEE Trans. Power Delivery* 29, 1, 414–421.

[13] Gomis-Bellmunt, O., Liang, J., Ekanayake, J., King, R., and Jenkins, N. 2011. Topologies of multiterminal HVDC-VSC transmission for large offshore wind farms. *Electric Power Systems Research* 81, 2, 271–281.

[14] John Graham, Abhay Kumar, and Geir Biledt. 2005. *HVDC Power Transmission for Remote Hydroelectric Plants*. https://search.abb.com/library/Download.aspx?DocumentID=9AKK101130D1764&LanguageCode=en&DocumentPartId=&Action=Launch.

[15] Kim, J.-H., Kim, C. H., Pothavajhala, V., and Pamidi, S. V. 2013. Current Sharing and Redistribution in Superconducting DC Cable. *IEEE Trans. Appl. Supercond.* 23, 3, 4801304.

[16] Kontos, E., Pinto, R. T., Rodrigues, S., and Bauer, P. 2015. Impact of HVDC Transmission System Topology on Multiterminal DC Network Faults. *IEEE Trans. Power Delivery* 30, 2, 844–852.

[17] Kumar, A. and Hussain, D. M. A. 2018. HVDC (High Voltage Direct Current) Transmission System: A Review Paper. *GJECS* 4, 2, 1–10.

[18] Lu, T., Zhao, S., and Cui, X. 2007. Simulation of Electromagnetic Induction on DC Transmission Lines from Parallel AC Transmission Lines. In *International Symposium on Electromagnetic Compatibility, 2007*. *EMC 2007 ; 23-26 Oct. 2007, Qingdao, China*. IEEE, Piscataway, NJ, 114–117. DOI=10.1109/ELMAGC.2007.4413444.

[19] Lutz, J., Schlangenotto, H., Scheuermann, U., and Doncker, R. D. 2018. *Semiconductor power devices*. *Physics, characteristics, reliability*. Springer, Cham, Switzerland.

[20] Madhan Mohan, D., Panigrahi, B. K., and Singh, B. 2009. Harmonic optimised 24-pulse voltage source converter for high voltage DC systems. *IET Power Electronics* 2, 5, 563–573.

[21] Manuel Reta-Herna´ndez. 2006. *Power system stability & control- transmission line parameters*. https://www.unioviedo.es/pcasielles/uploads/proyectantes/cosas_lineas.pdf.

[22] Mardiana, R. 2011. Parameters affecting the ampacity of HVDC submarine power cables. In *2011 2nd International Conference on Electric Power and Energy Conversion Systems*. IEEE, Piscataway, 1–6. DOI=10.1109/EPECS.2011.6126847.

[23] Meah, K. and Ula, S. 2007. Comparative Evaluation of HVDC and HVAC Transmission Systems. In *2007 IEEE Power Engineering Society General Meeting, Tampa, FL 24-28 June, 2007*. IEEE Xplore, Piscataway, N.J., 1–5. DOI=10.1109/PES.2007.385993.

[24] Mohan, N. 2011. *Electric power systems*. *A first course / Ned Mohan*. Wiley; Chichester : John Wiley [distributor], Hoboken, N.J.

[25] Oni, O. E., Davidson, I. E., and Mbangula, K. N.I. 2016. A review of LCC-HVDC and VSC-HVDC technologies and applications. In *2016 IEEE 16th International Conference on*

Environment and Electrical Engineering (EEEIC). *7-10 June 2016, Florence, Italy : conference proceedings*. IEEE, Piscataway, NJ, 1–7. DOI=10.1109/EEEIC.2016.7555677.

[26] Padiyar, K. R. 1990. *HVDC power transmission systems: technology and system interactions*. https://books.google.de/books?hl=en&lr=&id=gSoDaumDrjoC&oi=fnd&pg=PA21&dq=power+transmission+systems:+technology+and+system+interactions.&ots=rKewdvRY1O&sig=Op1SOc0mGwewqsDY4kYsBZbq3Qk&redir_esc=y#v=onepage&q=power%20transmission%20systems%3A%20technology%20and%20system%20interactions.&f=false

[27] Pieter de Jong. 2017. *Forecasting, integration, and storage of renewable energy generation in the Northeast of Brazil*. https://www.researchgate.net/publication/319991149_Forecasting_integration_and_storage_of_renewable_energy_generation_in_the_Northeast_of_Brazil/figures.

[28] Praça, A., Arakaki, H., Alves, S.R., Eriksson, K., Graham, J., and Biledt, G. 1996, May. *Itaipu HVDC transmission system 10 years operational experience*.

[29] Preece, R. 2013. *Improving the Stability of Meshed Power Networks*. *A Probabilistic Approach Using Embedded HVDC Lines*. Springer Theses, Recognizing Outstanding Ph. D. Research. Springer, Cham.

[30] Raza, A., Younis, M., Liu, Y., Altalbe, A., Rouzbehi, K., and Abbas, G. 2020. A Multi-Terminal HVdc Grid Topology Proposal for Offshore Wind Farms. *Applied Sciences* 10, 5, 1833.

[31] Ren, H., Zhong, L., Liu, M., Yu, Q., Li, Y., Zhao, W., and Zhou, Z. 2018. Effects of degassing duration on space charge and DC conductivity in HVDC XLPE cable insulation. In *2018 12th International Conference on the Properties and Applications of Dielectric Materials (ICPADM)*. IEEE, [Place of publication not identified], 124–127. DOI=10.1109/ICPADM.2018.8401118.

[32] rjanecek. Thyristor Catalog_2008-07-07.pdf.

[33] Roberto Rudervall, J.P. Charpentier, and Raghuveer Sharma. March 2000. High Voltage Direct Current (HVDC) Transmission Systems Technology Review Paper (March Jul. 2000).

[34] ScienceDirect. *Static Var Compensators - an overview | ScienceDirect Topics*. https://www.sciencedirect.com/topics/engineering/static-var-compensators. Accessed 14 December 2019.

[35] Slater, M., Schultz, A., Jones, R., and Fischer, C. *The-prediction of electromagnetic fields generated by submarine power cables*.

[36] softschools. *Magnetic Field Formula*. http://www.softschools.com/formulas/physics/magnetic_field_formula/343/. Accessed 22 December 2019.

[37] Sood, V. K. 2004. *HVDC and FACTS controllers*. *Applications of static converters in power systems*. Kluwer Academic Publishers, New York.

[38] Sun, Q., Wu, J., Lv, H., Wang, L., Han, W., Min, J., Zhang, Q., Li, Y., and Li, X. 2017. Analysis of coupling characteristics of hybrid electric field in the 750kV HVAC and ± 800kV HVDC parallel transmission lines. In *Proceedings of 2017 IEEE 5th International Symposium on Electromagnetic Compatibility (EMC-Beijing)*. *October 28-31, 2017, Beijing, China*. IEEE Press, Piscataway, NJ, 1–5. DOI=10.1109/EMC-B.2017.8260378.

[39] Tang, J., Zeng, R., Ma, H., He, J., Zhao, J., Li, X., and Wang, Q. 2007. Analysis of Electromagnetic Interference on DC Line From Parallel AC Line in Close Proximity. *IEEE Trans. Power Delivery* 22, 4, 2401–2408.

[40] University of Durban-Westville. 2003. *A study of high voltage direct current conductor corona in a purpose built corona caage*.

[41] Vahid Behravesh, N. A. New Comparison of HVDC and HVAC Transmission system.

[42] Weedy, B. M. 2012. *Electric power systems*. John Wiley & Sons, Chichester, West Sussex, UK.

[43] Wilson, C., George, C., and Steve, S., Eds. 2009. *Space charge accumulation under the effects of temperature gradient on solid dielectric DC cable*. *Cape Town, South Africa, 24 - 28 August 2009*. South African Inst. of Electrical Engineers, Cape Town.

[44] Wu, B. 2010. *High-power converters and AC drives*. Wiley, Hoboken, N.J, Chichester.

[45] Xiao, F., Yan, J., Zhang, B., and Wang, Y. 2018. Simplified approach of maximum electric field distribution on the ground near HVAC–HVDC shared tower transmission lines. *The Journal of Engineering* 2018, 17, 1851–1854.

[46] Xiong, Z., Fang, J., and Zhang, B. 2018. Simulation and Analysis of Magnetic Field in HVDC Transmission Cable. *IOP Conf. Ser.: Mater. Sci. Eng.* 382, 32041.

[47] Yogambal Jayalakshmi and S N Deepa. 2016. *Modelling of electric and magnetic fields under high voltage AC transmission line*.

[48] Bahrman, Michael; Johnson, Brian (2007): The ABCs of HVDC transmission technologies. In *IEEE Power and Energy Mag.* 5 (2), pp. 32-44. DOI: 10.1109/MPAE.2007.329194.

[49] Tan, C. Z. (2014): Radial electric potential in a metallic wire carrying a steady current. In *Optik* 125 (16), pp. 4333–4335. DOI: 10.1016/j.ijleo.2014.03.029.

[50] Eland cables, UK: ACSR conductors technical specifications. Available online at https://www.elandcables.com/media/38193/acsr-astm-b-aluminium-conductor-steel-reinforced.pdf.